

# Chapter 2

## Lithium Iron Phosphate (LiFePO<sub>4</sub>) as High-Performance Cathode Material for Lithium Ion Batteries



Neethu T. M. Balakrishnan, Asha Paul, M. A. Krishnan, Akhila Das,  
Leya Rose Raphaez, Jou-Hyeon Ahn, M. J. Jabeen Fatima,  
and Raghavan Prasanth

### Contents

2.1	Introduction .....	38
2.1.1	Emergence of Lithium Iron Phosphate .....	40
2.2	Synthesis of Lithium Iron Phosphate .....	41
2.3	Approaches for Property Enhancement .....	43
2.3.1	Carbon Coating .....	43
2.3.2	Metal–Metal Oxide Coating .....	45
2.3.3	Composite Electrodes .....	48
2.3.4	Doping .....	63
2.3.5	Size and Morphology .....	65
2.4	Conclusion and Future Outlook .....	66
	References .....	67

**Abstract** As long as the energy consumption is intended to be more economical and more environment friendly, electrochemical energy production is under serious consideration as an alternative energy/power source. Among different energy/power storage devices, lithium-ion batteries (LIBs) are currently the best commercially available devices. However, there are safety issues to be investigated even when it is operating at room temperature since there have been various incidents

---

N. T. M. Balakrishnan · A. Paul · A. Das · L. R. Raphaez · M. J. Jabeen Fatima (✉) ·  
R. Prasanth (✉)

Department of Polymer Science and Rubber Technology (PSRT), Cochin University of Science  
and Technology (CUSAT), Cochin, India  
e-mail: [jabeen@cusat.ac.in](mailto:jabeen@cusat.ac.in); [prasanth@cusat.ac.in](mailto:prasanth@cusat.ac.in)

M. A. Krishnan

Department of Mechanical Engineering, Amrita Vishwa Vidyapeetham, Kollam, India

J.-H. Ahn

Department of Chemical and Biological Engineering and Engineering Research Institute,  
Gyeongsang National University, Jinju-Daero, Republic of Korea

© The Editor(s) (if applicable) and The Author(s), under exclusive licence to  
Springer Nature Switzerland AG 2021

S. Rajendran et al. (eds.), *Metal, Metal-Oxides and Metal Sulfides for Batteries, Fuel  
Cells, Solar Cells, Photocatalysis and Health Sensors*, Environmental Chemistry for  
a Sustainable World 62, [https://doi.org/10.1007/978-3-030-63791-0\\_2](https://doi.org/10.1007/978-3-030-63791-0_2)

reported. From that point of view, effective research has been going on to develop LIBs that are viable to operate safely at higher temperatures. In the search for better cathode materials for LIBs, researchers have been investigating a new class of iron-based compounds called polyanions such as  $(\text{SO}_4)^{2-}$ ,  $(\text{PO}_4)^{3-}$  or  $(\text{AsO}_4)^{3-}$ . Orthorhombic  $\text{LiFePO}_4$  (LFP), which has an ordered olivine structure, has attracted particular interest due to its high-power capability, non-toxicity, and thermal stability. This material has relatively high theoretical capacity of  $170 \text{ mAhg}^{-1}$  when compared with other cathode materials. The major drawbacks of the lithium iron phosphate (LFP) cathode include its relatively low average potential, weak electronic conductivity, poor rate capability, low  $\text{Li}^+$ -ion diffusion coefficient, and low volumetric specific capacity. Hence, this chapter clearly emphasizes the role and progress of LFP as efficient cathode material for LIBs and their ways to overcome the existing drawbacks which include the optimization of their synthesis methods, controlling the diffusion rate, and modification strategies. The use of conventional electrolytes with LFP caused iron dissolution on the cathode surface, which catalyzed the electrolyte decomposition, which then contributed to the formation of thick obstructive solid electrolyte interphase (SEI) films. Use of electrolyte additives is one of the most effective methods to protect against  $\text{LiFePO}_4$  dissolution. The thermal stability of these materials can be accounted by the high  $\text{Li}^+$  ion diffusion rate and the electron transfer activity. Even at elevated temperatures up to  $340^\circ\text{C}$ , charged LFP and electrolyte didn't show any kind of chemical reactions, which makes this material thermally more feasible than other cathode materials like  $\text{LiCoO}_2$ ,  $\text{LiNiO}_2$ , and  $\text{LiMn}_2\text{O}_4$ .

**Keywords** Lithium ion batteries · Lithium iron phosphate · Carbon nanotube · Graphene · Cathode materials · Charge–discharge · Cycling stability

### List of Symbols and Formulas

$(\text{AsO}_4)^{3-}$	arsenate ion
$(\text{PO}_4)^{3-}$	phosphate ion
$(\text{SO}_4)^{2-}$	sulfate ion
$\text{Al}_2\text{O}_3$	aluminum oxide
$\text{C}_2\text{H}_2$	acetylene
$\text{CH}_3\text{COOLi}$	lithium acetate
$\text{CuO}$	copper oxide
$\text{Fe}_2\text{P}$	iron phosphide
$\text{Fe}(\text{CH}_3\text{COO}_2)_2$	iron acetate
$\text{FeC}_2\text{O}_4$	ferrous oxalate
$\text{FeOCl}$	iron oxychloride
$\text{FeOOH}$	ferric oxyhydroxide
$\text{FePO}_4$	iron phosphate
$\text{FePO}_4(\text{H}_2\text{O})_2$	iron phosphate hydrate
$\text{FePS}_3$	iron phosphorus sulfide
$\text{HCl}$	hydrogen chloride
$\text{Li}_2\text{CO}_3$	lithium carbonate

Li <sub>4</sub> Ti <sub>5</sub> O <sub>12</sub>	lithium titanium oxide
LiCoO <sub>2</sub>	lithium cobalt oxide
LiF	lithium fluoride
LiFePO <sub>4</sub>	lithium iron phosphate
LiMn <sub>2</sub> O <sub>4</sub>	lithium manganese oxide
LiNi <sub>0.5</sub> Mn <sub>0.5</sub> O <sub>2</sub>	lithium nickel manganese oxide
LiNiMnCoO <sub>2</sub>	lithium nickel manganese cobalt oxide
LiOH	lithium hydroxide
MgO	magnesium oxide
NH <sub>4</sub> H <sub>2</sub> PO <sub>4</sub>	ammonium dihydrogen phosphate
SiO <sub>2</sub>	silicon oxide
ZrO <sub>2</sub>	zirconium oxide

### Abbreviations

1-D	one-dimensional
2-D	two-dimensional
3D	three-dimensional
CNS	carbon nanospheres
CNT	carbon nanotubes
CUO	copper oxide
CVD	chemical vapor deposition
EG	ethylene glycol
EV	electric vehicle
GNS	graphene nano sheets
GO	graphene oxide
HEV	hybrid electric vehicle
LCO	lithium cobalt oxide
LFP	lithium iron phosphate
LIB	lithium ion batteries
LTO	lithium titanium oxide
MWCNT	multi-walled carbon nanotubes
PAN	poly (acrylonitrile)
PEG	polyethylene glycol
Ppy	polyvinyl pyrrolidone
PVA	polyvinyl alcohol
PVDF	polyvinylidene difluoride
rGO	reduced graphene oxide
SEI	solid/electrolyte interphase
SEM	scanning electron microscope
SWCNT	single walled carbon nanotubes
TEM	tunneling electron microscope

## List of Units

A g <sup>-1</sup>	Ampere per gram
C	C- rate
cm <sup>2</sup> s <sup>-1</sup>	Centimeter square per second
°C	Degree Celsius
eV	Electron volt
g mol <sup>-1</sup>	Gram per mole
h	Hours
kW kg <sup>-1</sup>	Kilo watt per kilogram
m <sup>2</sup> g	Meter square gram
mAh g <sup>-1</sup>	Milli ampere hour per gram
mA g <sup>-1</sup>	Milli ampere per gram
nm	Nanometer
Ω	Ohm
S cm <sup>-1</sup>	Semen per centimeter
V	Volt
Wh kg <sup>-1</sup>	Watt hour per kilogram

## 2.1 Introduction

Today's world is at a turning point where there is a decline in resources that leads to a new scenario in energy consumption. It is essential to find a suitable substitute that can ensure the surveillance of our wealth and development on long-term basis in order to face the run out of fossil fuel energy sources. In spite of careful consideration given to renewable energy over the non-renewable energy, their production and efficiency cannot be guaranteed, so effective storage of energy from these sources is important. Fuel cells, supercapacitors, and batteries are some of the important energy storage systems under research. Among them, batteries attract greater interest due to their efficiency and portability. So, batteries have an indispensable role in our daily life. They can be connected in series to get high voltage and parallel to get high current, and that is the wonder behind the battery technology.

The range of current batteries extends from non-rechargeable alkaline batteries to rechargeable lithium ion batteries (LIBs) and among these LIB technology currently attracts great interest owing to the electric vehicle revolution, because compared to other energy storage devices Li<sup>+</sup>-ion technology could serve as most effective power source for the automotive vehicle that can replace most of the gasoline technology (Ruska and Kiviluoma 2011; Cano et al. 2018). LIBs have an excellent combination of power as well as energy density. The lowest reduction potential of Li<sup>+</sup>-ions that authorizes highest cell potential, gravimetric and volumetric capacity as well as power density are the direct results by of the light weight and smallest ionic radii. Apart from this, the low self-discharge and lack of memory effect make it promising

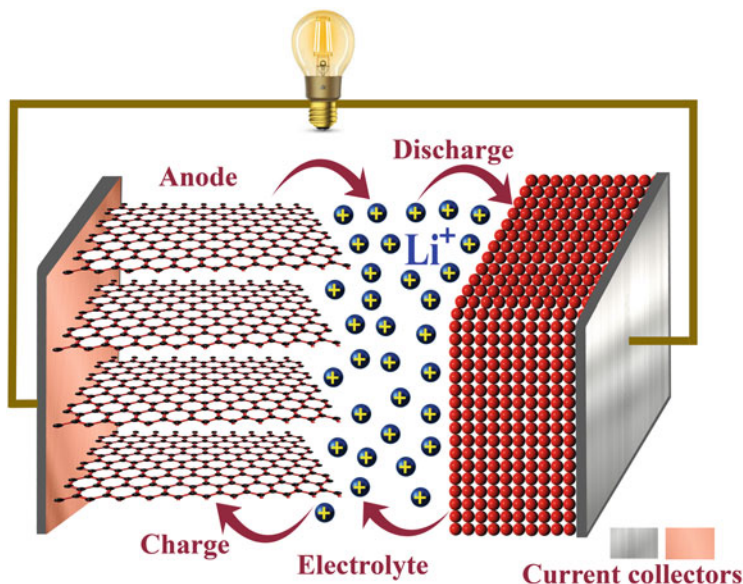


**Fig. 2.1** Schematic representation and operating principles of Li-ion batteries including the movement of ions between electrodes during charge and discharge states

candidate over other battery technologies such as lithium cadmium batteries (Li-Cd), nickel metal hydride battery (Ni-MH) (May et al. 2018). Also for these systems priming is not required. Low maintenance, low self-discharge (<5% for a month), and availability in varieties of shapes and sizes make LIBs superior over any other types of battery systems (Lu et al. 2013; Blomgren 2017).

An efficient and safer LIB was developed and commercialized after the successful safety test in 1985 by Akira Yoshino. At that time, he used lithium as the anode and vapor phase grown carbon fiber as the cathode material (Goodenough 2018). The typical schematic representation of lithium ion battery is given in Fig. 2.1. For efficient battery storage, an ideal cathode and anode are still remaining as a desire for the researchers. The first intercalation material discovered was titanium disulfide (TiS<sub>2</sub>) by Whittingham in 1975 (Whittingham 2012). But severe issues were related to cathode materials that produce lithium dendrite along with the metallic lithium anode and the titanium disulfide, which was expensive as well as forms hydrogen sulfide on exposure to air, which creates environmental issues (Whittingham and Gamble 1975). After that there comes the desire for an intercalation cathode material with higher intercalation potential of about >3 V.

The discovery of lithium cobalt oxide (LiCoO<sub>2</sub> simply LCO), the layered material as the cathode, by John Goodenough and Koichi Mizushima made a leap and it is known as the heart of LIBs. An intercalation compound is a type of material that is able to accommodate the guest Li<sup>+</sup>-ions in its layers and it can easily release the Li<sup>+</sup>-ions when needed. LCO was the most successful layered transition metal oxide cathode commercialized by SONY in 1991 and still it is used in many commercial

LIBs (Mizushima et al. 1981; Goodenough 2018). LCO exhibits high specific capacity ( $272 \text{ mAhg}^{-1}$ ) and high theoretical volumetric capacity ( $1363 \text{ mAhcm}^{-3}$ ). The high cost of cobalt made LCO expensive and as a toxic material it poses environmental issues. Low thermal stability and fast capacity fade are another issues associated with LCO. The major issue associated with the LIB is the thermal runaway during their application that is evident from the issue that led to the grounding of Boeing 787 airplanes in 2013, and explosion of electronic gadgets such as Samsung Note 7 (2017) and Samsung edge (2018) (Naoki et al. 2015). Several reports on electric vehicle explosion were reported worldwide. Chevrolet Volt was blasted while subjected to crash test in 2011. In 2013, Tesla Model S caught fire at Washington highway which was reported to be the worst case of explosion since the fire was inextinguishable with water. Later it was examined that dry fire extinguishers were found effective in putting out fire. In subsequent months, several incidents on explosion of Tesla model S were reported in Europe. This was also a reason for exploring new and efficient materials as cathodes. Lithium nickel oxide ( $\text{LiNiO}_2$  simply LNO) was considered as an alternative with similar structure of LCO, low cost but not efficient, because it has the tendency to replace  $\text{Li}^+$ -ion sites and thereby blocks the lithium diffusion. Continuous efforts led to the development of a new cathode material, lithium manganese oxide ( $\text{LiMn}_2\text{O}_4$ ,  $\text{Li}_2\text{MnO}_3$  simply LMO) in 1983, but still the tendency of the material to change structure from intercalation type to spinel during lithium extraction was a serious issue. This Jahn-Teller deformation reduces the capacity irreversibly on repeated cycling (Padhi 1997). After that, different intercalation type cathodes were developed, such as lithium nickel manganese oxide ( $\text{LiNi}_{0.5}\text{Mn}_{0.5}\text{O}_2$  simply NMO), lithium nickel cobalt manganese oxide ( $\text{LiNiMnCoO}_2$ , simply NMC), lithium titanate/lithium titanium oxide ( $\text{Li}_4\text{Ti}_5\text{O}_{12}$  simply LTO), that satisfactorily performed compared to the former.

### ***2.1.1 Emergence of Lithium Iron Phosphate***

The limitations of reported intercalation cathodes motivated the investigation for new type of cathode materials, out of which iron-based compounds were widely accepted owing to their properties. Initially studied compounds were iron phosphorus sulfide ( $\text{FePS}_3$ ), iron oxychloride ( $\text{FeOCl}$ ), and ferric oxyhydroxide ( $\text{FeOOH}$ ), which exhibited low discharge voltage, and they were found to be inadequate as cathode materials. The research was then focused on compounds containing polyanions such as  $(\text{SO}_4)^{2-}$ ,  $(\text{PO}_4)^{3-}$ , or  $(\text{AsO}_4)^{3-}$  (Padhi 1997; Takahashi et al. 2002). The use of lithium iron phosphate ( $\text{LiFePO}_4$  simply LFP) as cathode material in LIBs was first proposed by Akshaya Padhi, John Goodenough and his co-workers in 1996 (Padhi 1997; Rao 2015). It was the first ever reported cathode material with lower cost and abundance compared to LCO. It is olivine structured material with combination of plenty of Fe and covalent  $(\text{PO}_4)^{3-}$  units with fixed number of oxygen (Nishimura et al. 2010).

The major reason for the market acceptance of LFP is its superior properties such as thermal stability, safety, and specific capacity; however, it possesses certain drawbacks such as poor electronic conductivity and capacity retention under continuous charge–discharge cycling, especially at higher C-rate. While considering the safety aspects of LIBs, compared to small portable devices, the chances of catching fire is severe in electric vehicles (EVs), but the phosphate containing cathodes provide good thermal stability, so that it is able to withstand high temperatures and primarily stable during overcharged and short-circuiting conditions. Charging of LIB is also crucial above 4.7 V, since the formation of oxidative products or lithium deposition at high potential. So the choice of phosphate containing cathodes, such as olivine structured LFP, is completely safer even at high potential that it produces ferric oxide as the oxidative product, which is much more stable (Saw et al. 2014). Apart from this, LFP is the cathode material that provides low toxicity, flat potential during charge–discharge cycling process, and it provides high specific capacity. Also, LFP exhibits theoretical energy density of about 550 WhKg<sup>-1</sup>. It exhibits a theoretical specific capacity of 170 mAhg<sup>-1</sup>. So, the choice of LFP as the cathode material is even more satisfactory while considering the electrochemical performance as well as safety aspects of LIBs (Yang et al. 2002). Hence recent studies of cathode materials are mainly focused on LFP containing polyanions such as (SO<sub>4</sub>)<sup>2-</sup>, (PO<sub>4</sub>)<sup>3-</sup>, or (AsO<sub>4</sub>)<sup>3-</sup> (Padhi 1997). However, deterioration in capacity with cycle life and intolerance in high current is a problem with this material, so different studies are ongoing in order to meet excellent electrochemical properties and to reach extreme temperature performance (Dhindsa et al. 2013a; Lung-Hao Hu et al. 2013).

## 2.2 Synthesis of Lithium Iron Phosphate

Synthesis methods of LFP can be divided broadly into two types, mainly solid-state methods and solution phase methods. Solid state methods include solid phase synthesis, mechano-chemical activation, carbothermal reduction, and microwave heating, that usually results the formation of powder state LFP. Solid state synthesis is the conventional method for the synthesis of LFP. LiF, Li<sub>2</sub>CO<sub>3</sub>, LiOH·2H<sub>2</sub>O, CH<sub>3</sub>COOLi, etc. are used as lithium sources, FeC<sub>2</sub>O<sub>4</sub>·2H<sub>2</sub>O, Fe(CH<sub>3</sub>COO<sub>2</sub>)<sub>2</sub>, and FePO<sub>4</sub>(H<sub>2</sub>O)<sub>2</sub> are used as the iron sources, and NH<sub>4</sub>H<sub>2</sub>PO<sub>4</sub> and (NH<sub>4</sub>)<sub>2</sub>HPO<sub>4</sub> are used as the phosphorus sources. The process takes place at extreme condition that results in the formation of non-crystalline particle in non-crystalline form. Islam et al. (2015) synthesized LFP by solid state method using low cost material. In mechano-chemical activation method (Bağcı and Akyildiz 2018), as its name indicates, mechanical activation is done in order to enhance the chemical reaction and it results in the formation of smaller particles with high activation energy. In comparison with solid state methods, carbothermal reduction method produces fine LFP particles with uniform particle morphology and high capacity. Microwave heating (Park et al. 2003) includes heating of the material by making use of microwave

energy, hence it is more productive and less energy consuming process. Solution-based techniques get much attention compared to solid state method, because it results in small particle size, more uniform particle size distribution, higher purity, and better electrochemical performance. Hydrothermal synthesis, sol-gel synthesis, spray pyrolysis, and co-precipitation are the widely used solution techniques for the production of LFP.

During the hydrothermal synthesis of LFP (Qin et al. 2010), pure platelets are formed. It is the simple, clean, and low-cost method widely used, which involves the boiling of a solution of precursors above the boiling point of water, typically 150 °C. It is the synthesis method that enables more control over the particle size and particle size distribution. Normally hydrothermal synthesis is a high energy consuming process. Benedek et al. (2017) introduced a low temperature hydrothermal process with the use of high concentration of precursors. They produced LFP platelets with (010) dimension and practical capacity of 150 mAhg<sup>-1</sup>. For the preparation of nano LFP, a hydrothermal synthesis via solution stirring is employed, that results in cathodes with good capacity retention (Gariépy et al. 2012).

Sol-gel synthesis involves the formation of a sol, which get converted in to gel that consists of interconnected rigid skeleton with pores, made of colloidal particles. It is a low-cost process that doesn't require any high temperature conditions. It results in phase pure LFP with uniform morphology and good control over the particle size as well as it is possible to induce in situ carbon coating using suitable precursor or solvents (Yang and Xu 2004). LFP synthesized using a natural iron stone precursor along with Li<sub>2</sub>CO<sub>3</sub> powder and NH<sub>4</sub>H<sub>2</sub>PO<sub>4</sub> powder with dilute HCl as solvent exhibit an electronic conductivity of about 4.56 × 10<sup>-3</sup> Scm<sup>-1</sup>, which is six times greater than that of pure LFP (Angela et al. 2017).

Ultrasonic spray pyrolysis is the effective method that results in the formation of ultra-fine particles with narrow size distribution. It involves the formation of continuous droplets from a solution containing precursor colloids. The process starts with spraying of solution of mixed precursor in the form of droplets to the pyrolysis furnace followed by calcination at high temperature (Yang et al. 2006). LFP/C composite that is prepared by the same method exhibits a first discharge capacity of 140 mAh g<sup>-1</sup> at 0.1 C, and excellent cyclic performance (Konarova and Taniguchi 2008). Effect of carbon precursors on LFP/C composites shows that sucrose is one of the best carbon precursors for LFP in ultrasonic spray pyrolysis (Kashi et al. 2018).

Co-precipitation method forms LFP well-crystallized powders by mixing lithium and phosphate compounds in a mixed precursor solution. Co-precipitated slurries are then filtered, washed, and dried (Huang et al. 2013). Depending on the precursors and other processing conditions, the size of LFP can be varied from nano to micro size (Li et al. 2009; Ding et al. 2010). An environmentally benign co-precipitation method was introduced by Swider et al. (2014) by synthesizing technical grade reagent in ethylene glycol (EG) medium at an anhydrous environment that results in pure fine nano powder of LFP. But using ethylene glycol in aqueous solution for one step co-precipitation method results in the formation of LFP with excellent electrochemical properties (Wang et al. 2013).



## 2.3 Approaches for Property Enhancement

The major target of the research on LFP cathode was to improve the electronic conductivity of this active material. For achieving the required level of electronic conductivity several methods were chosen for modification of the structure and morphology of the LFP. Carbon coatings, doping with metallic impurities, constructing 3-D network frames with conducting materials such as carbon nanotubes, and graphene and particles size reduction or increase in the available active surface area for the electrochemical reaction are the important methods reported to improve the properties of LFP. The major refinements reported are discussed in detail. The enhancement of property is observed due to the formation of a conducting surface film, incorporation of the metallic impurities, addition of some metal dopants, formation of 3-D conducting channels, etc. But the problems with some of the dopants are that due to low solubility of dopant that they get located over the lithium site and they block the diffusion of Li<sup>+</sup>-ion (Fig. 2.2).

### 2.3.1 Carbon Coating

Carbon coating is considered as one of the simplest and powerful method to improve the electronic conductivity of LFP. The carbon coating was first proposed by Armand and his co-workers (Li and Zhou 2012). During the carbon coating, pyrolysis of an organic substance over the LFP occurs, which creates a reducing atmosphere that may result

in the formation of secondary phase, which enhances the electronic conductivity and enables to achieve a practical capacity value of 170 mAhg<sup>-1</sup> (Saroha and Panwar 2017). Carbon coating helps to inhibit the aggregation of nano particles and thereby provide the passage for Li<sup>+</sup>-ions, as well as the inter and intra particle

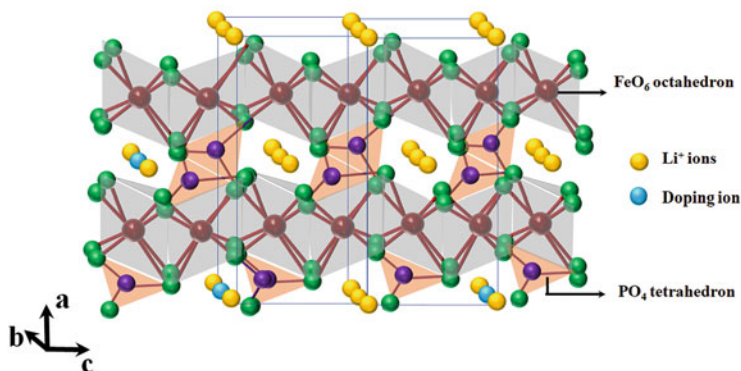


**Fig. 2.2** The schematic representation on diffusion of Li by obstruction of the channels, which degrades the electrochemical performance. (Modified after Julien 2017)

electronic conductivity. A thin layer of carbon was coated on nanosized LFP by pre-calcination and vacuum deposition process, which results into uniform particle size distribution, prevention of particle agglomeration, and inhibit the grain growth (Huang et al. 2017). In industrial scale, a high-performance carbon coating is achieved by coating 90 nm thick particle covering with 3 nm thick carbon coating. Carbon derived from different sources was used for coating process. Orange peel was introduced during the modified mechanical activation process. This carbon-coated LFP exhibits a high discharge capacity of about  $147.3 \text{ mAhg}^{-1}$ , which is 87% of the theoretical capacity at 0.5 C-rate (Kim et al. 2019).

A soft and hard carbon coating on LFP was prepared by using asphalt derived and glucose derived carbon and the electrochemical performances were evaluated. The variation study shows that the electrochemical property of soft carbon-coated LFP is greater than hard carbon-coated LFP. Asphalt is a good carbon precursor that could form uniform and denser carbon layer and thereby improve the  $\text{Li}^+$  diffusivity across the electrode–electrolyte interface as well as improve the electronic conductivity (Jiang et al. 2017). Acetylene gas is another precursor which is employed to introduce carbon coating on LFP via in situ pyrolysis. The  $\text{C}_2\text{H}_2$  treatment on LFP for 10 min shows excellent capacity at all C-rate studied (0.1–10 C) as well as superior rate performance (Saroaha and Panwar 2017).

Among the different processes employed for the synthesis of carbon-coated LFP, an effective method for carbon coating was proposed by Wang et al. (2011). They produced nanosized LFP with carbon coating using  $\text{FePO}_4$  as the iron source and polyvinyl alcohol (PVA) gel as the carbon source. The best film forming property of PVA makes a uniform film coating over the LFP particle after it gets mixed with the  $\text{FePO}_4$  in ball mill, and during calcination it perfectly gets transferred into the uniform carbon coating. Electrospinning was also proposed as an effective method to grow LFP/C nanofibers. Poly (acrylonitrile) (PAN) is one of the carbon sources that provides the carbon coating during electrospinning. It offers a large surface area to volume ratio and provides a capacity value of  $162 \text{ mAhg}^{-1}$  at 0.1 C-rate. It is a better performance compared to other LFP/C nanofibers and the carbon content in the coating is found to be about 10 wt.% (Shao et al. 2013; Lin et al. 2014; Qiu et al. 2014a). The morphology of  $\text{LiFePO}_4/\text{C}$  composite synthesized at different mole ratio is depicted in Fig. 2.3. The variation in molar concentration was achieved by changing the precursor concentration in  $\text{LiH}_2\text{PO}_4/\text{FeC}_6\text{H}_5\text{O}_7$  of mole ratio 1.0–1.3 with regular increment of 0.1, out of which 1.3 mole ratio showed superior performance. Apart from this, the composite exhibits superior electrochemical performance than commercial LFP (Fig. 2.4) (Qiu et al. 2014b).

Hydrothermally synthesized LFP nano rods that are coated using sucrose precursor exhibit a capacity value of about  $173 \text{ mAhg}^{-1}$  at 0.1 C, which is greater than the theoretical value. This excellent improved property is due to the reduction of the lithium path along the (010) direction which is most favorable for  $\text{Li}^+$  diffusion (Bao et al. 2017). Solution deposition followed annealing is also employed for the formation of carbon-coated LFP nanostructures, which showed that annealing over  $700^\circ\text{C}$  results in the reduction of  $\text{LiFePO}_4$  to  $\text{FePO}_4$ . The reduction from  $\text{LiFePO}_4$  to  $\text{FePO}_4$  is favorable for the enhanced electronic conduction (Zhu et al. 2014). Apart

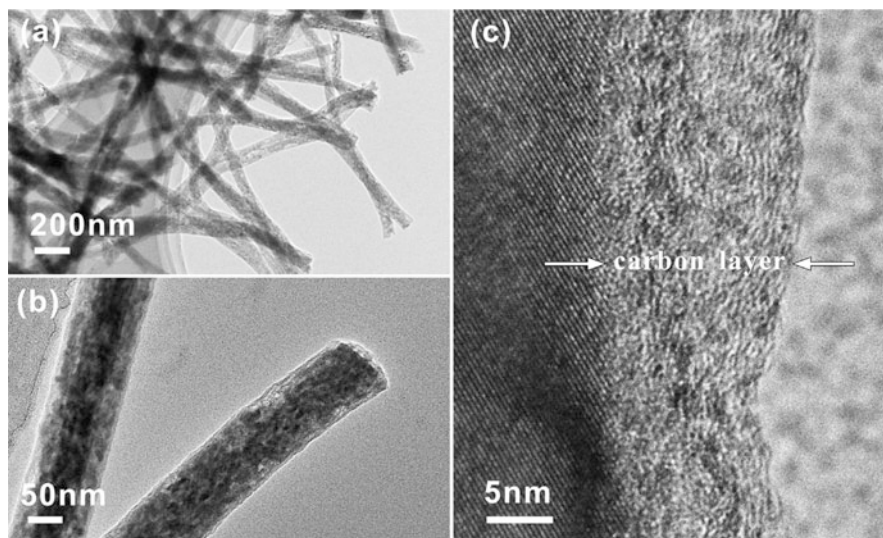


**Fig. 2.3** TEM images of LiFePO<sub>4</sub>/C composite nanofibers prepared using LiH<sub>2</sub>PO<sub>4</sub>/FeC<sub>6</sub>H<sub>5</sub>O<sub>7</sub> ratio of 1.3 with different magnifications. (Reprinted with permission of Elsevier from Qiu et al. 2014b)

from the effect of carbon layer formed on the active material (LFP) during carbon coating, the role of interface conductivity between carbon-coated LFP particle and carbon-coated current collector were studied. In this study, LFP prepared by sol-gel method and a nanosized thin layer of carbon was coated on the active materials and the electrode was fabricated on carbon-coated aluminum which produces highly distorted carbon at the interface. The sample containing more sp<sup>2</sup> hybridized carbon exhibits superior electrochemical properties over sp<sup>3</sup> hybridized carbon. This is due to the large polarization effect during the charge—discharge cycle (Swain et al. 2015).

### 2.3.2 Metal–Metal Oxide Coating

Among the different approaches introduced for the enhancement of rate capability and power density of LIBs, particle size reduction and carbon coating get much attention by the battery technologists; however, carbon coating cannot ensure a complete uniform coating on the active surface of LFP particles. When there is a barrier for the movement of electrons, the intercalated Li<sup>+</sup>-ions remain as such and it will create polarity in the electrode. For different active cathodic materials such as LCO and LTO, different metal coatings like MgO, ZrO<sub>2</sub>, Al<sub>2</sub>O<sub>3</sub>, and SiO<sub>2</sub> were effectively employed in order to improve the electronic conductivity (Zhao et al. 2017).

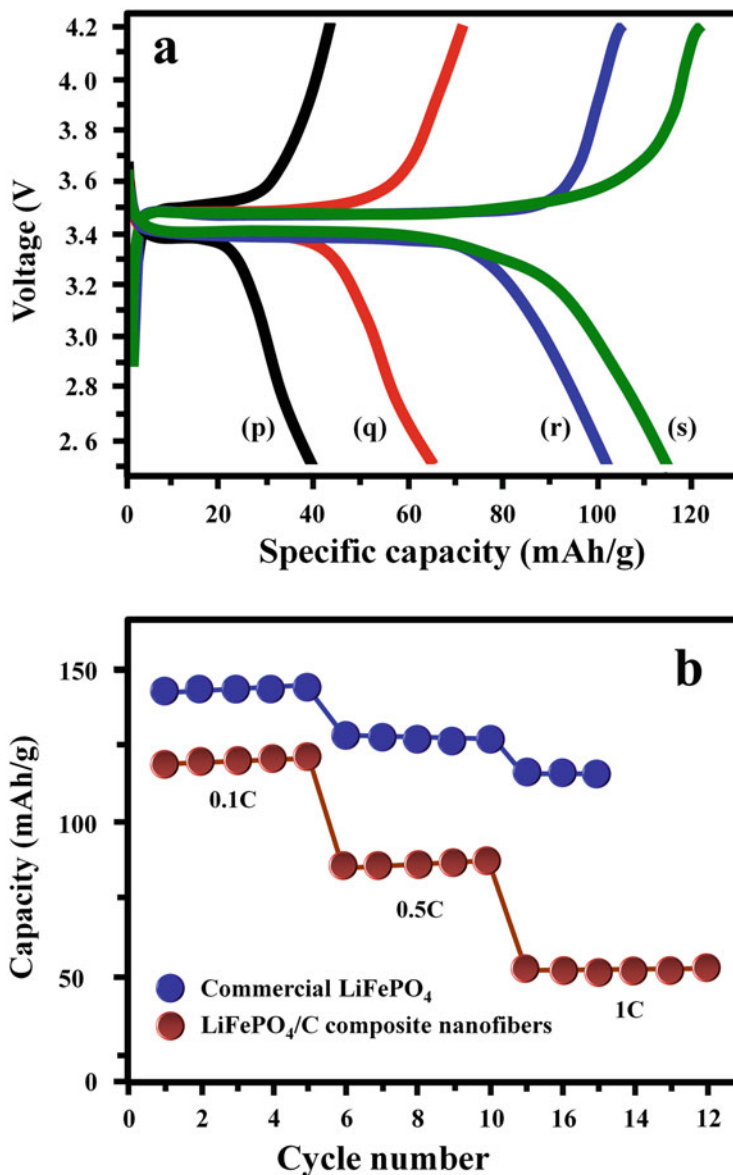


**Fig. 2.4** (a) Charge/discharge curves of  $\text{LiFePO}_4/\text{C}$  composite nanofiber samples prepared using different mole ratio of  $\text{LiH}_2\text{PO}_4/\text{FeC}_6\text{H}_5\text{O}_7$ : (p) 1.0; (q) 1.1; (r) 1.2; (s) 1.3. (b) Capacity of commercial  $\text{LiFePO}_4$  and  $\text{LiFePO}_4/\text{C}$  composite nanofibers at different discharge rate of 0.1, 0.5, and 1 C. (Cell configuration:  $\text{LiFePO}_4/\text{C}$  composite nanofibers/Li cells). (Reprinted with permission of Elsevier from Qiu et al. 2014b)

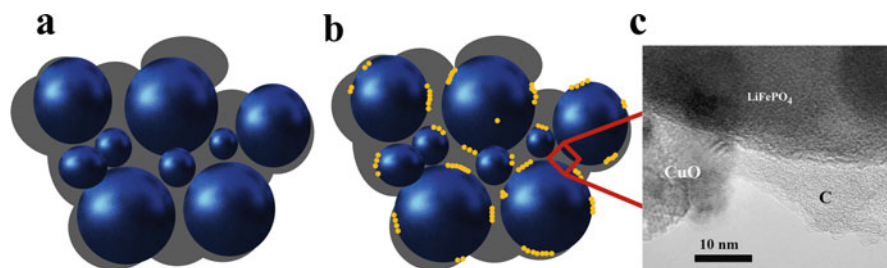


**Fig. 2.5** Schematic representation of LiFePO<sub>4</sub> particles: (a) partially coated with carbon, (b) designed ideal structure of LiFePO<sub>4</sub> particles coated with an integrate nanolayer, (c) HRTEM images of the CuO/C-LFP. (Reprinted with permission of Elsevier from Cui et al. 2010)

In LFP, nanosized CuO and carbon are together employed for coating, and this nano CuO cover up the incomplete carbon layer network and forms a metallic nano layer over the surface of LFP (Fig. 2.5). CuO coating was carried out with chemical vapor deposition and it results in the formation of an integrated and continuous conducting metallic layer on the active material. Compared to carbon-coated LFP, this system exhibits improved discharge capacity, 125 mAhg<sup>-1</sup> (Cui et al. 2010). Another study of LTO modified carbon-coated LFP shows that compared to simply carbon-coated LFP, modified carbon-coated LFP exhibits high cyclic stability even when the cell was operating at a higher temperature like 55 °C. A solid-state method is employed in order to synthesize LFP/C powder and 1–5% LTO was applied by using the spray drying process. Compared to LTO coated LFP, pristine LFP shows a decline in cycling stability and about 3 wt.% LTO was optimized for the best electrochemical properties of LFP (Yang et al. 2015).

In the carbon-coated LFP, a spherical phase growth is observed which completely differs from that of pure matrix phase and this growth was reported to be owing to the formation of a conducting Fe<sub>2</sub>P phase which was first reported by Herle et al. (2004). The report also examined the influence of carbon coating for the formation of Fe<sub>2</sub>P phase and the layer formed is controlled by the size, temperature, and annealing atmosphere of LFP (Liu et al. 2018).

Formation of a uniform carbon layer over LFP increases the Li<sup>+</sup> diffusion and electronic conductivity. SiO<sub>2</sub> is a non-metallic oxide that improves the structural stability of the LFP/C by insulating the LFP surface effectively from the electrolyte. An improved structural stability and reduced interfacial resistance increase the Li<sup>+</sup> diffusivity (Li et al. 2011). Similarly zinc oxide (ZnO) coating is also employed which greatly helps to attain the high reversible capacity (about 90% of that of theoretical capacity of the active material), when cycled between 2.5 and 4.2 V. ZnO coating by freeze drying method also showed an enhanced electrochemical performance of LFP, which is assigned to the semiconducting nature of ZnO.

### 2.3.3 Composite Electrodes

The fabrication of composite electrodes was another major modification approach carried out in LFP in order to enhance the conductivity and efficiency of the electrode in LIBs. It can be done by coating of the surface of LFP via chemical or physical route.

#### Lithium Iron Phosphate-Carbon Nanotube Composite Cathode

Discoveries of very stable nanometer size  $sp^2$  carbon bonded materials such as fullerenes, nanodiamonds, carbon nanotube (CNT), and graphene are enhanced the research in nanocomposites. A new era in carbon materials begins with the discovery of Buckminster Fullerene's family (Bucky Balls) (Kroto et al. 1985) at Rice University, United States in the mid of 1980s, followed by the discovery of Fullerene nanotubes (Bucky tubes by Sumio Iijima and Ajayan Pulickal) (Iijima et al. 1992), and large scale synthesis of carbon nanotubes by Ajayan and Ebbesen (1992). CNTs, the allotrope of carbon, having a seamless tubular structure, are dimensionally and structurally different from other allotrope of carbon like graphite, diamond, fullerene, and graphene. These are one-dimensional (1-D) materials having very high aspect ratio (length to diameter ratio) of up to 132,000,000:1, significantly larger than for any other nanostructured materials. They can be thought of as one atom thick flexible sheets of carbon called graphene, rolled up at specific and discrete (chiral) angles into a long and hollow structures basically categorized into two: (i) single walled carbon nanotubes (SWCNTs)—this can be visualized as cylinder composed of a rolled up graphene nanosheets around a central hollow core; (ii) multi-walled carbon nanotubes (MWCNTs). It consists of more than one graphene layers, that is held together by Van der Waals forces between adjacent layers and folded as hollow cylinders (Salem et al. 2003). The combination of rolling angle and radius decides the properties of CNTs, for instance, whether the individual nanotube shell is metallic, semiconducting, or insulating in nature (Fig. 2.6.).

The way graphene nanosheets are rolled can be described by a pair of indices ( $n, m$ ), where  $n$  and  $m$  represent number of unit vectors along the two directions of hexagonal crystal lattice of graphene. The chirality of CNTs is defined by chiral vector,  $C_h = na_1 + ma_2$  when  $m = 0$ , CNTs have zig-zag structure for  $n = m$  arm chair structure, and if both conditions are not satisfied, it is classified as chiral (Thostenson et al. 2001). The electronic property of CNTs greatly depends on the chirality. For a given pair of indices ( $n, m$ ), if  $(2n + m)$  is a multiple of 3, then the CNTs are metallic in nature, otherwise semiconductor. Figure 2.6 depicts (a) SWCNT, (b) MWCNT, and (c) their unit vectors. The ( $n, m$ ) nanotube naming scheme can be thought as a vector ( $C_h$ ) in an infinite graphene sheet that describes how to "roll up" the graphene sheet to make the nanotube.  $T$  denotes the tube axis,  $a_1$  and  $a_2$  are the unit vectors of graphene in real space.

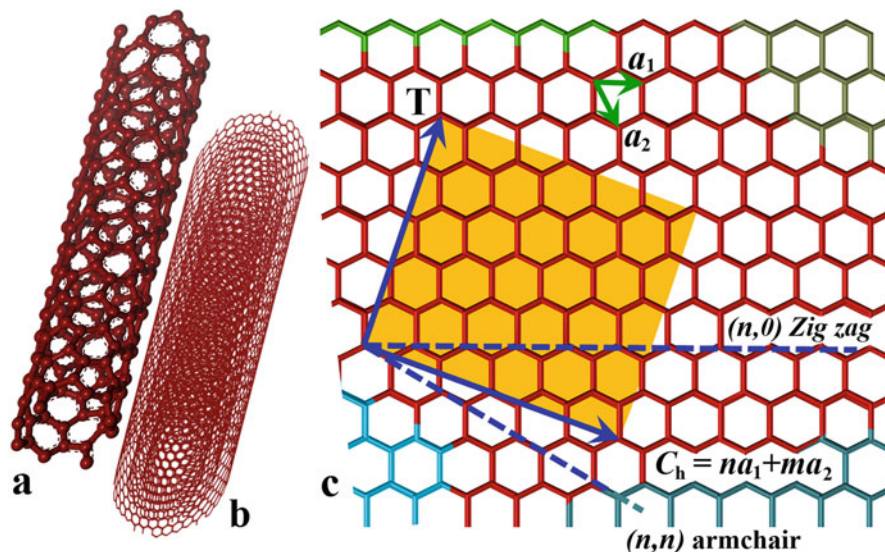


**Fig. 2.6** Schematic illustration of (a) SWCNT, (b) MWCNT, and (c) its unit vectors. The  $(n,m)$  nanotube naming scheme can be thought of as a vector ( $C_h$ ) in an infinite graphene sheet that describes how to “roll up” the graphene sheet to make the nanotube.  $T$  denotes the tube axis, and  $a_1$  and  $a_2$  are the unit vectors of graphene in real space. (Modified after Jabeen et al. 2015)

The characteristic electronic and electrochemical properties of CNTs are being identified as an ideal material for energy storage devices such as batteries, supercapacitors, and fuel cells. Among these devices, considerable number of efforts are being reported to make composite electrodes with lithium transition metal oxides such as LCO and LFP, for the development of high-performance LIBs. Due to the p-orbital overlap in metallic CNT chiralities, easy conduction of electrons can occur via ballistic transport (i.e., the electrons can transport with mean free path on the order of microns along the length of nanotube unless scattered by a defect). This type of property exceptionally improves the specific capacities, C-rate performance, and cyclic stability when used as an additive with active materials, particularly in conjunction with the poor transport inherent to cathode materials like LFP.

The large specific surface area, good transport properties, and cage like more accessible structure of CNTs for Li insertion are useful for the development of high performance and flexible electrodes for LIBs. Recent literature shows the ability to maintain about 10% improvement in reversible capacity at low rates up to 3 C-rate for LCO and 5 C-rate for LFP (Landi et al. 2009). For any cathode material, intercalation of ion and electron transport properties are very critical for high performance. Carbon nanotubes exhibit very high electrical conductivity in axial direction, and due to their particular structure, free electrons are distributed in the surface of CNTs, which help them displace randomly (Jin et al. 2008). A novel network made from LFP particles mixed with CNTs is being studied for high rate capabilities. The networks consisting of CNTs interconnect the LFP particles, which

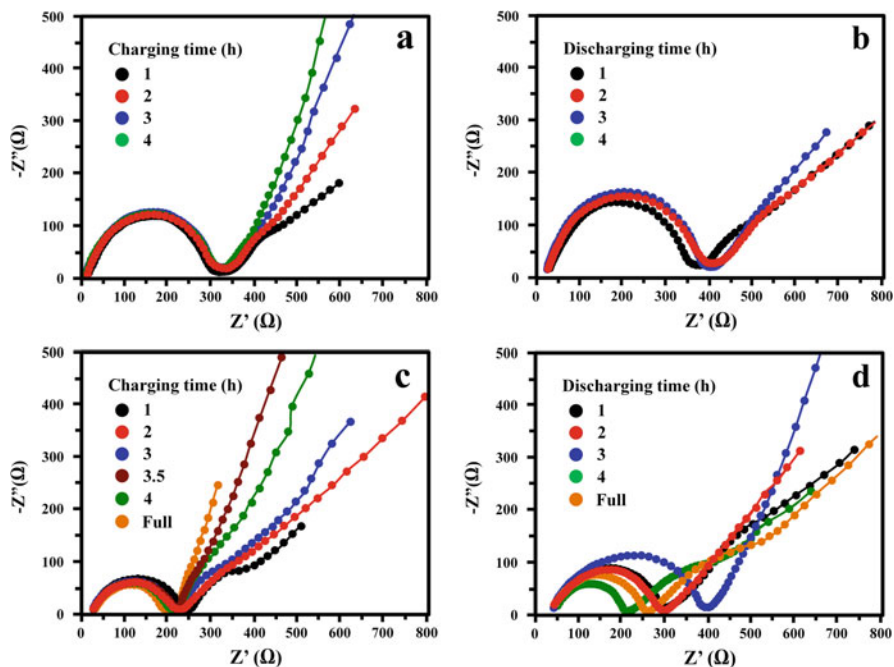


**Fig. 2.7** Electrochemical impedance spectra of cathodes: (a) Non- modified LiFePO<sub>4</sub>, (b) Non modified LiFePO<sub>4</sub>, (c) CNTs-modified LiFePO<sub>4</sub>, (d) CNTs-modified LiFePO<sub>4</sub>. (Reprinted with permission of Elsevier from Chen et al. 2010)

effectively enhance the electron transfer between the active material and current collector. The impedance slope of LFP/CNT composite studied by using electrochemical impedance microscope is very high, indicating enhanced electrochemical activity of LFP due to CNT network (Fig. 2.7). When comparing the non-modified LFP and CNTs-modified LFP, the resistance of charge transfers at high frequency drops sharply in all states. This shows that the state of charge has null effect on charge transfer resistance. From this, it can be concluded that CNTs have immense role in accelerating the charge transfer. There is a spontaneous increase in the charge transfer resistance from the state of charge to discharge. A substantial divergence is being perceived in the state of discharge. With this process of discharge, the resistance of charge transfer dwindles. This will be the reason for the enhancement of electronic conductivity and increase in contact efficiency between the particles of CNTs-modified LFP cathode that lessen the charge transfer resistance. The fall of resistance helps the improvement in performance, thus giving the major contribution for the excellent electrochemical performance of CNTs-modified LFP at high rate (Chen et al. 2010).

CNT-modified LiFePO<sub>4</sub> evince exceptional performance in terms of both specific capacity and cycle life. The increase in electronic conductivity adversely increases the specific capacity and cyclic life of LFP. Both SWCNTs and MWCNTs are



effectively used in order to enhance the electrochemical performance of LFP. The modification of LFP with MWCNT evinces the electronic conductivity of LFP due to the formation of 3D network wiring. The addition of MWCNTs to LFP results in high capacity with fast rate and high efficiency. MWCNTs prepared by hydrogen arc discharge method in normal atmosphere and room temperature when incorporated with LFP showcased better charge-discharge cycling behaviors than LFP with acetylene black at the same amount of content respectively. The specific area of acetylene black is 92 m<sup>2</sup>/g, which is very much larger than that of MWCNTs, which have a surface area of 71 m<sup>2</sup>/g. The acetylene black has many oxo-functional groups and micropores on the surface that affect the electrochemical performance of LFP, which is being tackled by the introduction of CNTs- to LFPs (Li et al. 2007).

There are many methods of synthesis of CNT-modified LFP, like hydrothermal process, sol-gel synthesis, solid-state reactions, spray drying method, two step solution method, polyol process, electrospinning, and chemical vapor decomposition. In hydrothermal process, the CNTs are being coated with the help of high temperature in aqueous solution with high vapor pressure. Usually the construction of 3-D network of LFP/CNT, in which CNTs coat and connect the LFP nanoparticles, synthesized by hydrothermal process is being assisted by ethylene glycol. The presence of EG can limit the growth of LFP particles and help in the development of homogeneous structure. Very high initial discharge capacity, capacity retention, and rate capability are exhibited. The particle size of LFP, synthesized by hydrothermal method with the assistance of EG, is very small and thus improve the electronic conductivity performance of battery (Feng et al. 2017). This method of synthesis on large scale can enhance the manufacturing of batteries with higher rated capacity, which is useful for automotive industry for electric vehicles (Thanh et al. 2018). An attractive application of CNT-modified LFP proposed by adding a low fraction of graphene displays substantial increase in current density and Li<sup>+</sup> diffusion (Chen et al. 2018). Another study revealed that mesoporous 3-D CNT-modified LFP microsphere (Fig. 2.8) embedded homogeneously not only increase electronic conductivity, but also facilitate the penetration of electrolyte into the microstructure which was synthesized by polyethylene glycol (PEG)-assisted method using different molecular weight of PEG (400, 1500, and 20,000 gmol<sup>-1</sup>). The morphology of samples are displayed in Fig. 2.9 (Tan et al. 2014) Among the different samples the composite microsphere fabricated with 400 molg<sup>-1</sup> PEG showed enhanced electrochemical performance with a capacity retention of 95.7% even at 5 C after 100 cycles (Fig. 2.10).

Another method of synthesis for CNT composite is chemical vapor decomposition, where the CNTs-modified LFP synthesized by this method significantly enhances the electrochemical performance. By this method, CNT is coated uniformly on LFP grains and this improves the quality of the cathode (Tian et al. 2015). CNTs-modified LFP nanoplates composite cathode with graphene sheets (GS) by one-step polyol process under low temperature has been studied and found that CNTs are evenly distributed among LFP particles. Also the cross-linked CNTs penetrate through or embed into the LFP particles. In addition, the CNTs and GS inter-weaving tightly with each other thus form a 3-D network throughout the

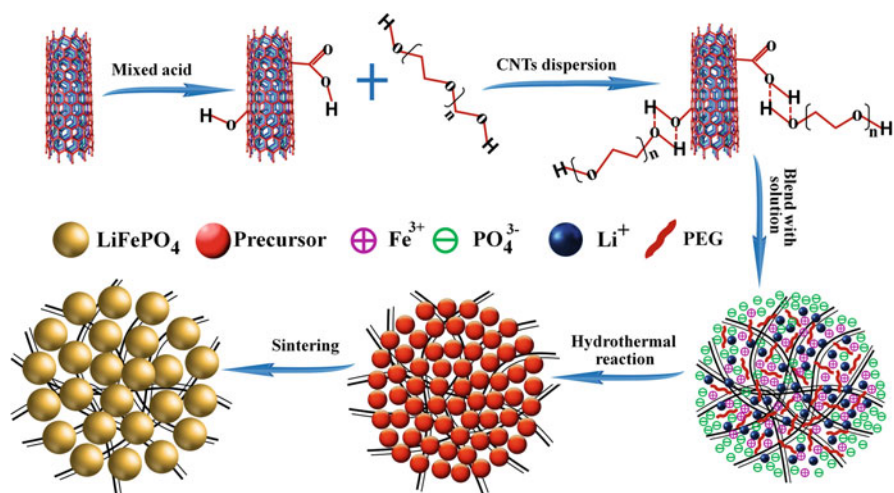


**Fig. 2.8** Schematic illustration of the formation process of the porous LFP/CNTs microsphere. (Reprinted with permission of Elsevier from Tan et al. 2014)

composite materials. This distinctively conductive network were successfully incorporated, which supply more paths and accelerate the speed of electron transfer and  $\text{Li}^+$ -ion diffusion in the composite. The electrochemical studies showed that the addition of CNTs led to the increase in specific capacity of LFP. The CNT-modified LFP synthesized by polyol process exhibit cycling profiles smoother than that of pristine LFP, indicating better cycling stability and superior reversibility of  $\text{Li}^+$ -ion insertion/extraction reactions of the composite (Wu et al. 2013a). CNT decorated with LFP and carbon has been reported by Wu et al. (2013b) in which they have obtained a low temperature performance at  $-25^\circ\text{C}$  and high temperature performance at  $120^\circ\text{C}$ . The morphological studies reveal that the carbon-coated LFP/CNT composite exhibits a single crystalline nature (Fig. 2.11) and show higher capacity retention at higher C-rate and cycling stability in both low and high temperatures (Fig. 2.12).

Carbon nanospheres (CNS)-modified LFP composite prepared by sol-gel route produced desirable structure of olivine composite. Compared to CNT; CNS exhibit novel characteristics such as greater diameter, high surface area, and electronic conductivity. During the sol-gel synthesis rather than a uniform coating, an agglomeration of CNS particles is formed over the LFP surface. This reveals that the simple mixing of CNS and LFP cannot ensure the formation of network. Similar is the case for CNTs (Liu et al. 2010). An innovative and environment friendly CNT-modified LFP composite cathode was synthesized by sonication of Na-carboxymethyl cellulose in aqueous medium, which not only delivers high electrochemical performance, excellent charge storage capability, and cycling stability but also creates sufficient space between CNT particles that facilitate the faster electrolyte permeability, thus easy to wet the electrode leads to early stabilization of the cell. This in turn decreases

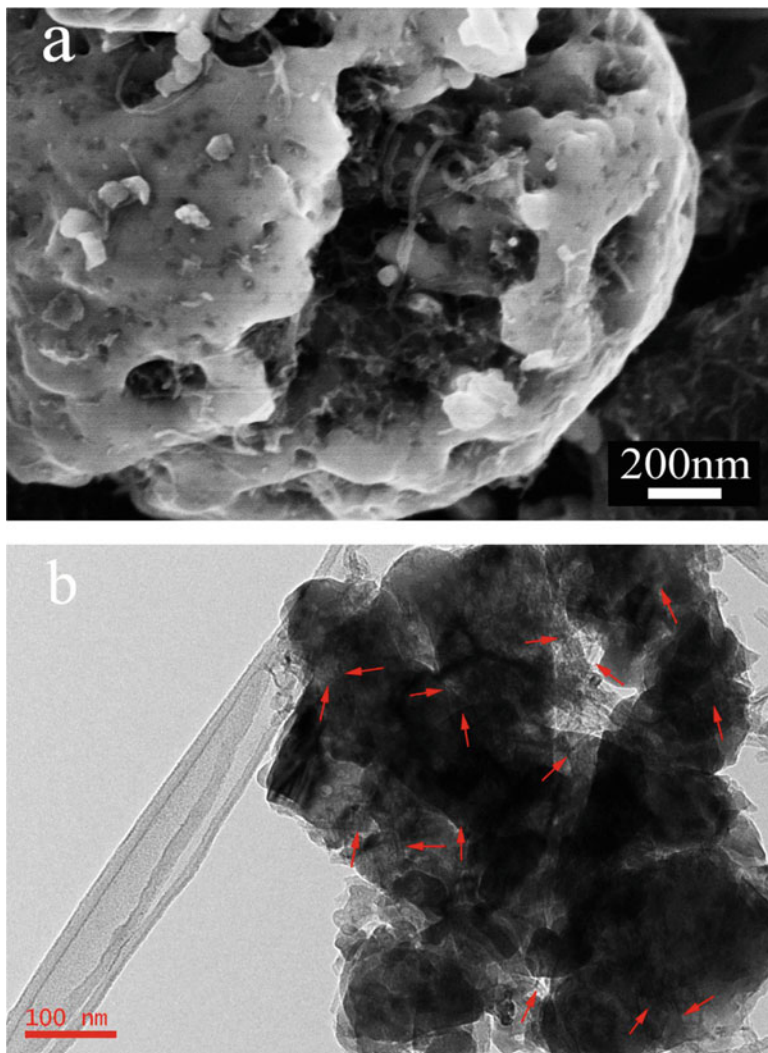


**Fig. 2.9** (a) SEM image, (b) TEM image of crushed M-LFP/CNTs-400 microspheres. (Reprinted with permission of Elsevier from Tan et al. 2014)

the concentration polarization when cathode is being subjected to high current loads. Besides the remarkable performance of battery, the great advantage of this is its environment friendly nature (Varzi et al. 2014). A hierarchical porous carbon-coated CNT-modified LFP microspheres composite is being experimented to enhance the properties of positive electrode. This method not only enhanced the electronic conductivity but also aimed to optimize the desired microstructure for accelerating mass transfer and enhance the tap density simultaneously. It has been found that the Li<sup>+</sup> transport in electrolyte toward the active site may also be limiting factor at high

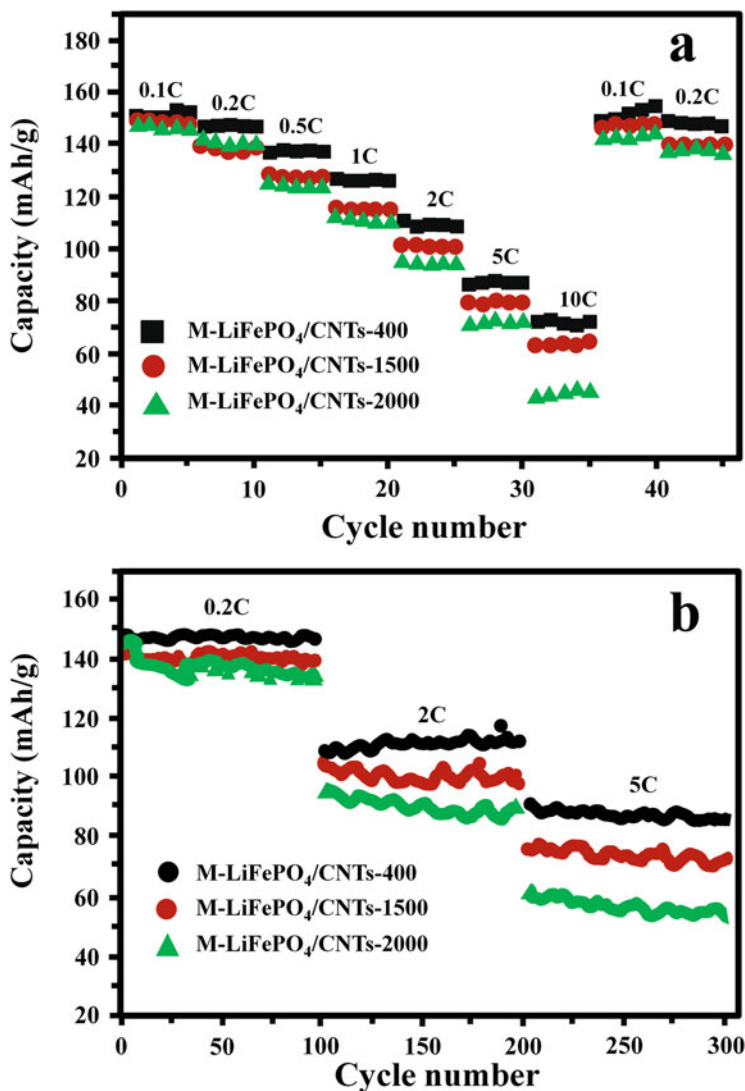


**Fig. 2.10** (a) Rate capabilities and (b) cycling performances of the M-LFP/CNTs-x composites. (Reprinted with permission of Elsevier from Tan et al. 2014)

rates, and tap density directly influence the volumetric energy densities in LIBs, which is an essential feature for electric vehicles (EVs) and hybrid electric vehicles (HEVs) (Wang et al. 2016).

The electrochemical performance of carbon-coated LFP/MWCNT composite cathode having micron size of LFP (100–200 nm) (Qin et al. 2014b) and nanosized LFP (40–90 nm) (Zou et al. 2013) were reported. LFP have a carbon coating of thickness of 1–3 nm using poly(acrylonitrile) (PAN) (Qin et al. 2014a) or sucrose

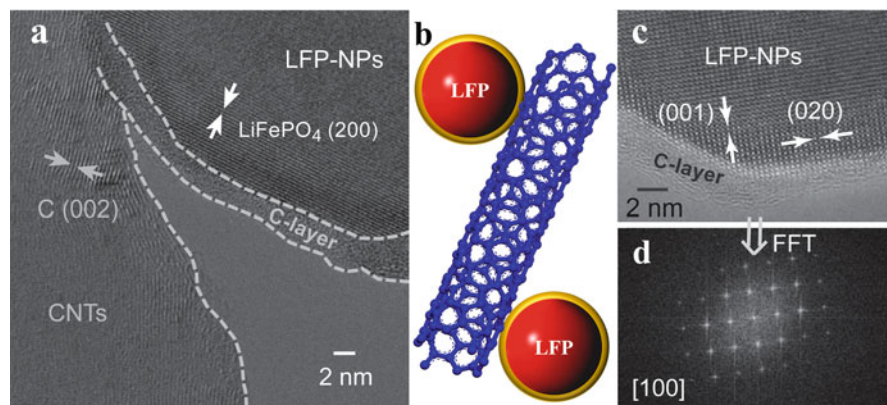


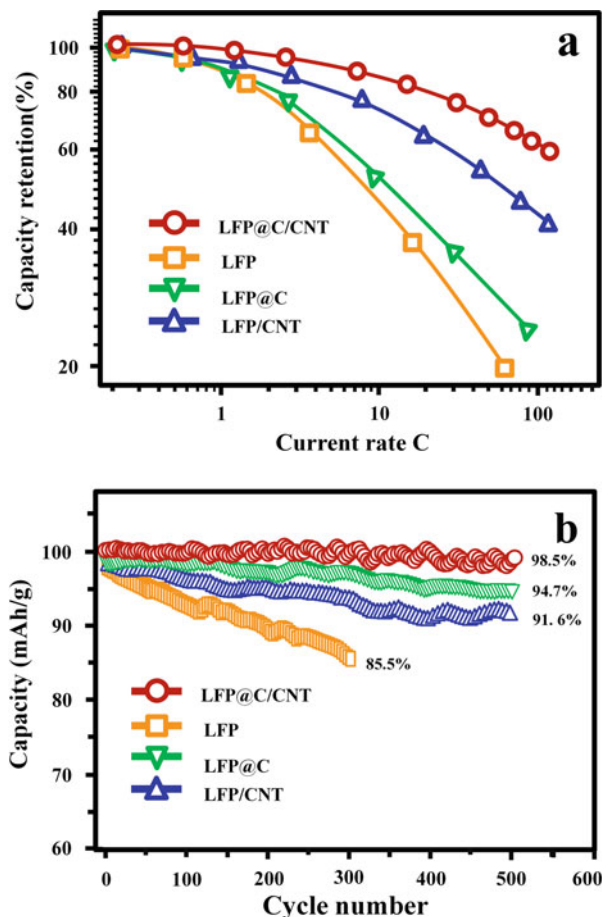
**Fig. 2.11** (a, c) HRTEM images of the prepared LFP@C/CNT nanocomposite; (b) schematic illustration of the prepared LFP@C/CNT nanocomposite; (d) the corresponding FFT pattern of the HRTEM in (c) (Reprinted with permission of John Wiley and Sons from Wu et al. 2013b)

(Wu et al. 2013c; Wang et al. 2016) as a carbon source. The electrical conductivity shown by C-LFP/MWCNT is  $2.3 \times 10^{-2} \text{ Scm}^{-1}$  (micron-sized LFP) and  $7.7 \times 10^{-2} \text{ Scm}^{-1}$  (nanosized LFP), which is much higher than the C-LFP or pristine LFP indicating that CNTs and amorphous carbon are the cause for the enhancement of electronic properties. The charge–discharge capacity of C-LFP/CNT is  $\sim 170 \text{ mAhg}^{-1}$  at a current density of 0.5 C and  $\sim 142 \text{ mAhg}^{-1}$  at 20 C with good capacity retention even at high C-rate (Qin et al. 2014a, b). The carbon-coated CNT-modified LFP exhibits superior electrochemical properties in terms of an ultra-high rate capability. For LIBs in electric vehicles, charging time is very important. It has been observed that the C-LFP/CNT cathode only took 142 s (20 C) for charging 76% of full charge capacity (Wang et al. 2016).

Qiao et al. (2017) reported LFP/CNT composite cathode exhibiting a high discharge capacity of  $123 \text{ mAhg}^{-1}$ . The LFP based composite cathode also evinced long cycling stability, which is prepared by using CNTs coated with polyvinylpyrrolidone (PVP). The composite cathodes obtained contain 3 wt. % CNT showed a high discharge capacity of  $123 \text{ mAhg}^{-1}$ . The cathode also exhibited a very low capacity fade of 1.6 and 20% up to 1000 and 3400 cycles respectively at a current density of 10 C. The loss in capacity in this study is four to eight times lower than that of previously reported LFP/CNT and LFP/graphene composite cathodes (Qiao et al. 2017). This superior rate capability and ultra-high cycling stability is accredited to the combined effect of the large  $\text{Li}^+$ -ion diffusion coefficient achieved in LFP nanoparticles by mixing with CNTs and the highly conductive 3-D framework of monodispersed CNTs, which is free from breaking and entangling effects (Qiao et al. 2017).

Electrospinning is an easy and versatile method of preparation of binder-free electrodes with fibrous morphology and controlled properties. The Fig. 2.13 shows schematic representation of an electrospinning set up for the preparation of metal

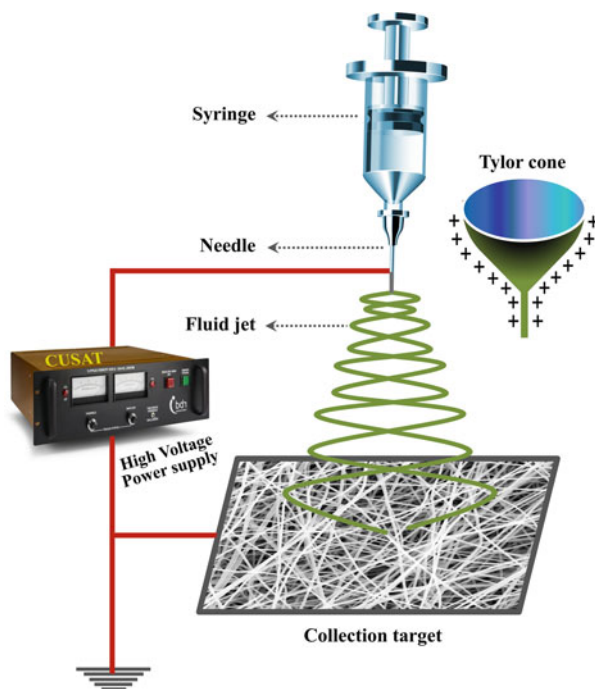
**Fig. 2.12** Comparisons of (a) rate capability and (b) cycling performances of LFP@C/CNT, LFP@C, LFP/CNT, and pristine LFP. (Reprinted with permission of John Wiley and Sons from Wu et al. 2013b)



oxide nanofibers. Toprakci et al. (2012) reported of the synthesis of LFP/CNT/C composite nanofibers by electrospinning and sol-gel method using CNT as functional filler and PAN as the medium for electrospinning and carbon source. The hybrid fibrous electrode evinces an initial reversible capacity of 150, 162, and 169  $\text{mAhg}^{-1}$  for pristine LFP powder LFP/C and LFP/CNT/C composite nanofibers respectively. The unique fibrous structure of LFP/CNT/C, high surface-volume ratio, complex porous structure, and shorter  $\text{Li}^+$ -ion diffusion pathway, enhance the electrode reaction kinetics and reduces the polarization, which in turn gives a good cycling stability, high reversible capacity, and high rate capabilities (Toprakci et al. 2012).

CNTs-modified LFP coated with carbonaceous materials (C/CNT-LFP) also received great attention as cathode materials in LIBs owing to their enhanced conductivity. C/CNT decorated LFP have been synthesized by polyol-based synthesis, which showed specific capacitance of  $160 \text{ mAhg}^{-1}$ . The samples also showed enhanced performance even at low temperature of  $-25^\circ\text{C}$  (Wu et al. 2013c). A 3D,

**Fig. 2.13** Schematic of typical electrospinning set up



porous, hierarchically modified C/LFP/MWCNT composite electrode was fabricated via in situ sol-gel method, showed enhanced electrochemical properties compared to the LFP and LFP/CNT electrodes. Modified C/LFP/MWCNT composite electrode delivers a power density of  $16.8 \text{ kWkg}^{-1}$  whereas for pristine LFP is  $12 \text{ kWkg}^{-1}$  and that of CNT/LFP is  $14 \text{ kWkg}^{-1}$ . Similarly, energy density of C/LFP/MWCNT composite electrode is much higher ( $84 \text{ Whkg}^{-1}$ ) compared to that of pristine LFP and CNT/LFP ( $60$  and  $70 \text{ Whkg}^{-1}$ ). The rate performance of C/LFP/MWCNT composite electrode was obtained about  $142 \text{ mAhg}^{-1}$  at  $20 \text{ C}$ -rate. At low C-rate C/10, it showed a capacitance of  $169.6 \text{ mAhg}^{-1}$ , which was almost equal to the theoretical capacity of LFP ( $170 \text{ mAhg}^{-1}$ ) (Qin et al. 2014a). The morphological studies (Fig. 2.14) showed a uniform carbon coating is formed over the porous LFP, which greatly contributes to the electrochemical properties (Fig. 2.15) and electronic conductivity of the composite material.

The electrodes in LIBs contain a large amount of inactive materials, which limit the specific capacity of LFP to  $120 \text{ mAhg}^{-1}$  from  $170 \text{ mAhg}^{-1}$ . There have been many attempts to eliminate these inactive components from LFP cathode by introducing a freestanding flexible cathode with super P and polyvinylidene difluoride (PVDF) binder and without super P or PVDF binder (Susantyoko et al. 2017). The freestanding electrode with 90 wt.% LFP at the current rate of  $170 \text{ mAg}^{-1}$  delivers a specific capacity of  $\sim 134 \text{ mAhg}^{-1}$  (Susantyoko et al. 2018), which is much higher than the specific capacity of  $\sim 79 \text{ mAhg}^{-1}$  at a current rate of  $127 \text{ mAg}^{-1}$  (about

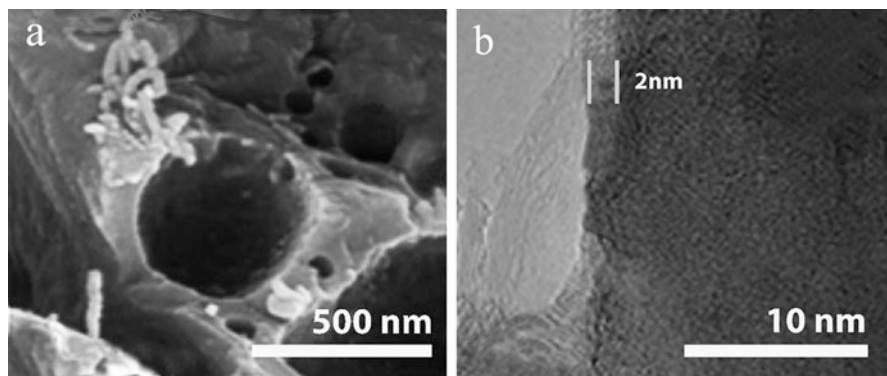
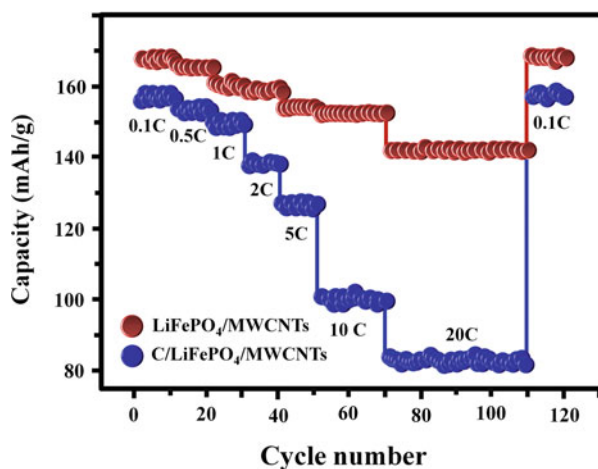


**Fig. 2.14** Morphology of LFP (a) SEM image of pure LFP, (b) HRTEM image of C/LiFePO<sub>4</sub>/MWCNT. (Reprinted with permission of Elsevier from Qin et al. 2014a)

**Fig. 2.15** The rate performance curves of MWCNTs modified LiFePO<sub>4</sub> materials at various current rates (0.1–20 C). Reprinted with permission of Elsevier from Qin et al. 2014a)



0.75 C-rate) reported in earlier study (Susantyoko et al. 2017). The difference in capacity is due to the different grade of MWCNT used in different studies.

### LiFePO<sub>4</sub>/Graphene Composite Electrode

The 2D sheets of carbon composed of sp<sup>2</sup> hybridized carbon atoms forming one atom thick planar sheet are known as graphene. It exhibits extraordinary properties such as high conductivity, mechanical stability, thermal stability and flexibility (Mao et al. 2012). It is the most strongest material which has been ever discovered (Papageorgiou et al. 2017). Incorporation of graphene with the metal oxides substantially enhances its electrochemical properties. The synergistic mechanism offered by this nanocomposite helps to deliver the properties of both graphene as



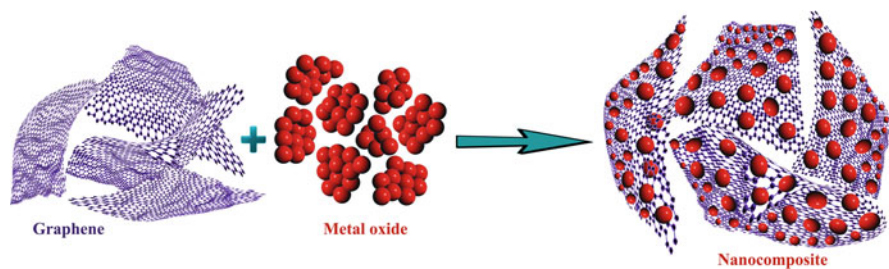


**Fig. 2.16** Schematic of the preparation of graphene/metal oxide composites with synergistic effects between graphene and metal oxides. (Modified after Wu et al. 2012)

well as the metal oxides (Fig. 2.16). This effect can be made use to enhance electrochemical properties of LFP, hence LFP/graphene composite electrode will substantially enhance the conductivity compared with pristine LFP electrode.

In recent past, a composite cathode of LFP with graphene and its nanostructures had been given much importance for its ability to enhance the electrochemical performance of LFP-based cathodes. The active material for use of cathode material is processed by the methods like, sol-gel, hydrothermal, or solid state reactions (Xu et al. 2007; Xiang et al. 2010). Until today, LFP/graphene composites are prepared by the simple methods such as sol-gel method (Yang et al. 2012), the solid state reactions (Wang et al. 2015b), the hydrothermal method (Wang et al. 2010; Zhang et al. 2012; Bo Wang et al. 2015a), co-precipitation method (Ding et al. 2010), and simple physical mixing. Ding et al. (2010) first reported a LFP/graphene composite having a specific capacity of 160 mAhg<sup>-1</sup> as compared to 113 mAhg<sup>-1</sup> for commercial LFP. Su et al. (2010) brought graphene into LFP as a planar conductive additive to give a flexible graphene based conductive network. These past studies conclude that even with a lower fraction of graphene additive (compared to commercial carbon-based additives such as CNT and CNF), the charge/discharge performance of the nanocomposite is superior to the pristine LFP. A conducting LFP/graphene composite was prepared using a facile hydrothermal method followed by heat treatment by Wang et al. (2010). and found that LFP particles attached to the surface of graphene or embedded in graphene nanosheets showed higher electronic conductivity and Li<sup>+</sup>-ion diffusion due to the formation of uniformly interconnected 3D conducting network of graphene nanosheets (Wang et al. 2010). Similar charge-discharge and cycling properties were reported for LFP/graphene nanocomposite synthesized in the ratio of 92:8. The LFP/graphene nanocomposite exhibited a discharge capacity of 160.3 mAhg<sup>-1</sup> at 0.1 C and 81.5 mAhg<sup>-1</sup> at 10 C (Wang et al. 2010). For further improvement, Y. Wang et al. (2012) prepared LFP/graphene nanocomposite by solid-state synthesis, 3-D porous LFP/graphene composite via sol-gel process (Yang et al. 2012), and simple mechanical mixing methods (Tang et al. 2012). The specific capacity of 161 mAhg<sup>-1</sup> at 0.1 C and 70 mAhg<sup>-1</sup> at 50 C (Wang et al. 2012) were reported for composite prepared by solid-state synthesis, whereas porous LFP/graphene composites evinced a capacity values of 45–60 and 75–109 mAhg<sup>-1</sup> without and with graphene respectively for a high rate of 10 C

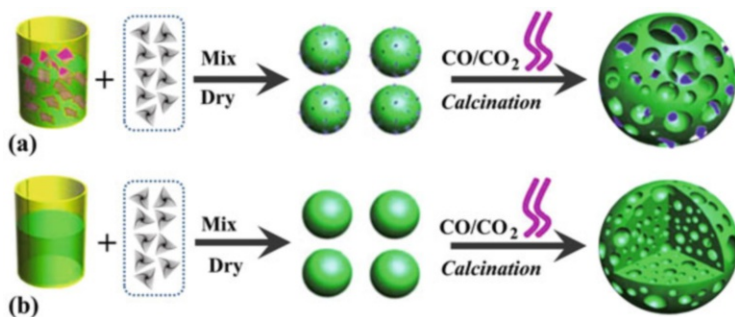


**Fig. 2.17** Schematic representation of formation of 3-D porous networks: (a) LFP/graphene and (b) LFP. (Reprinted with permission of Elsevier from Ma et al. 2013)

(Yang et al. 2012). The sol-gel method exhibited superior performance even at higher rates compared to other methods by mechanical mixing (Tang et al. 2012) and solid-state synthesis (Wang et al. 2012). Dhindsa et al. (2013b) used sol-gel method to prepare LFP/graphene nanocomposite to increase the electronic conductivity of LFP. Graphene oxide (GO) was mixed with LFP precursors for this study. The resulting composite improved the electron conductivity by six orders of magnitude compared to the pristine LFP (Dhindsa et al. 2013b). The uniformly sized LFP particles are covered by graphene nanosheet and form an interconnected 3-D conducting channel, which is responsible for high electronic conductivity. Additionally, a high specific capacity of  $160 \text{ mAhg}^{-1}$  was recorded, which is near to theoretical value limit, and excellent cycling stability was achieved. In order to reduce the distance of  $\text{Li}^+$  diffusion, three-dimensional nanoporous spheres within micron size regime are considered to be the optimal structure for LFP, capable of achieving high power capability without altering the packing density and facilitating the quick and efficient transport of ion and charge (Magasinski et al. 2010). LFP/graphene porous composites synthesized by a facile template-free sol-gel method (Yang et al. 2012) (Fig. 2.17) and facile precipitation method (Ma et al. 2013) were employed for two different studies. The reversible capacity of LFP/graphene ( $146 \text{ mAhg}^{-1}$  at  $17 \text{ mA} \text{g}^{-1}$ ) obtained is 1.4 times greater than that of porous LFP ( $104 \text{ mAhg}^{-1}$ ), demonstrating the incorporated graphene substantially enhances the specific capacity throughout the charge–discharge cycling process. It has also been noted that the porous LFP/graphene composite also shows a considerable tolerance to differing charge/discharge current densities. However, it is observed that the oversized holes fail to achieve the advantage of high tap density of porous structure, and no significant improvement on electrochemical performance is observed by the non-uniform distribution of graphene. Ma et al. (2013) prepared a  $\text{GO}/\text{Li}_3\text{PO}_4$  composite by precipitation process which was employed as a sacrificial template for the hydrothermal synthesis of porous graphene LFP composite. The LFP microspheres exhibited a uniform morphology, which are being wrapped by graphene nanosheets. The LFP/graphene cathodes deliver discharge capacities of 141, 130.9 and  $101.8 \text{ mAhg}^{-1}$  at current rates of 0.1, 1 and 10 C respectively due to

the formation of effective 3-D conducting network, formed by bridging of graphene nanosheets and the porous structure, which could absorb electrolyte to the interior of the LFP particles that help the easy diffusion of Li ions. The electrochemical studies showed that LFP/graphene nanocomposite material exhibits good rate capability, and displayed about 72% of the initial capacity at 10 C. The increase in performance is accredited to the porous LFP microsphere which exhibited a hierarchical structure assembled by nanoparticles, higher electronic conductivity, and chemical stability of graphene network in composite and porous structure in approval of Li ion diffusion (Ma et al. 2013).

By co-precipitation method of preparation of nanostructured LFP/graphene, composites in de-ionized water at room temperature was reported by Ding et al. (2010). In LFP/graphene composites, graphene nanosheets were used as scaffolds. There is a decrease in discharge capacity with higher C-rate, which is being accredited interfacial impedance offered to the Li<sup>+</sup>-ion diffusion at LFP and FePO<sub>4</sub> interface. The cycling stability and rate capability of LFP/graphene has been assured to the fact that nanosized particle with large surface area and improved electrical conductivity through the graphene nanosheets to increase the electronic conductivity and lowers the contact resistance between LFP and GNS (Ding et al. 2010; Chen et al. 2013). Yang et al. (2013) reported comparative study of electrochemical properties of folded and unfolded LFP/graphene nanocomposites. It is found that the composite electrode delivers good discharge capacity which is about 98% to the theoretical capacity (170 mAhg<sup>-1</sup>) and showcased a stable cycling behavior for 100 cycles. The composite electrode prepared with unfolded graphene was able to achieve high capacity due to efficient dispersion and restriction of size in nanoscale of LFP. The LFP particle easily attach with unfolded graphene and set a good interface between graphene nanosheets and LFP particles, thus increases the electronic conductivity (Yang et al. 2013). The LFP cathode with a specific capacity higher than theoretical value using carbon-coated LFP surface modified with 2 wt.% of electrochemically exfoliated graphene layer was reported by Hu et al. (Lung-Hao Hu et al. 2013). The composite cathode delivers a specific capacity of 208 mAhg<sup>-1</sup> without causing unfavorable voltage polarization. The composite cathode delivers a specific capacity of 208 mAhg<sup>-1</sup> without causing unfavorable voltage polarization. The enhanced conductivity exhibited by exfoliated graphene flakes wrapping around C-coated LFP helps fast electron transfer during the charge/discharge cycles, which in turn gives 100% Coulombic efficiency without fading at different current rates. The energy density is 686 Whkg<sup>-1</sup>, which is very much higher than the typical 500 Whkg<sup>-1</sup> of LFP. The graphene flakes which cover over the C-coated LFP exhibit high conductivity, diminishing the irreversible capacity at first cycle and thus giving ~100% Coulombic efficiency (Lung-Hao Hu et al. 2013). 3% graphene incorporated LFP composite cathode shows an initial discharge of 164 mAhg<sup>-1</sup> only owing to the grasping of Li<sup>+</sup>-ions by the multi-layer graphene films of LFP nanocomposite during the charge/discharge process (Wang et al. 2018). The synthesis of LFP/graphene composite was always found to be time consuming process. The motive behind this has always been to design an easy-to-use method and produced easily at low cost. Studies revealed that the best method for processing

LFP/graphene composite in terms of energy capacity is hydrothermal method with an efficiency of 97% of the theoretical value (Lei et al. 2014). The temperature in this method was being maintained at 180 °C for 10 h, the solution is cooled at room temperature, precipitated, centrifuged, washed in deionized water three times, dried under vacuum for 4 h, and finally sintered at 600 °C for 2 h under hydrogen/argon (5:95, v/v). This method also provided an easy pathway for electron transfer and Li<sup>+</sup> diffusion. Spray-drying is also an effective method for the preparation of LFP/graphene composite. Zhou et al. (Chem et al. 2011) studied the facile procedure by physical mixing of LFP and reduced graphene oxide (rGO) suspension when spray dried at 200 °C to be a solid LFP/graphene composite and annealed to form the LFP/graphene composite cathode. These LFP primary nanoparticles embedded in micron-sized spherical secondary nanoparticles were wrapped homogeneously and loosely with rGO sheets, thus forming a 3-D graphene network bridging between LFP. This structure is beneficial for fast electron transfer throughout the secondary particles, while the presence of ample voids between LFP nanoparticles and graphene sheets help for Li ion diffusion. This composite cathode exhibited high specific capacity and charging/discharging, cycling stability, and rate capability. The synergetic effect offered by the combination of nanosizing with organized conducting templates to provide an excellent electron transport for high power applications was being demonstrated by Sun et al. (Ha and Lee 2015). The study reported on a size-constrained in situ polymerization method to process core-shell C-coated LFP nanoparticles hybridized with rGO as a cathode for high-power LIBs. In order to prevent the spontaneous aggregation of hydrophobic graphene in a aqueous solution, hydrophilic graphene oxide was used as precursor during the formation of LFP/graphene composite via in situ polymerization of pyrrole. The fabrication of C-coated LFP/rGO hybrid cathode material is been accredited to three factors: (i) in situ polymerization of polypyrrole (Ppy) for constrained nanoparticle preparation of LFP, (ii) increase in dispersion of conducting 2-D networks endowed by colloidal stability of GO, and (iii) intimate film contact between the LFP and rGO nanosheets. The study evinced the importance of conducting template dispersion by different LFP/C-rGO composites in which an agglomerated rGO solution has been used as the starting template. The hybrid C-coated LFP/rGO cathodes exhibited superior rate capability and discharge capacity close to that of the theoretical capacity, thus increasing the electrochemical performance which is again accredited to the fast electron and Li<sup>+</sup>-ion transport through nanosized active materials (Ha and Lee 2015). Bi et al. (2013a) studied three methods to synthesize graphene by chemical vapor deposition (CVD), Wurtz-type reaction and chemical exfoliation (Bi et al. 2013a). The study claimed that the presence of graphene reduced the contact resistance between LFP particles, which enhanced the electronic conductivity of LFP. It also reported that LFP/graphene nanocomposite prepared with graphene by CVD is more efficient in terms of electronic conductivity, contact resistance, and electrochemical performance.

## LFP/Sulphur Cathodes

The performance of LFP can be enhanced by appropriate doping in the site of oxygen leading to anion doping (Liu et al. 2008). Sulfur being a same group element of oxygen with similar properties but with larger size makes the element suitable for anion doping in LFP to enhance the performance (Okada et al. 2018). The increase in size of the anion will enhance the rate de-intercalation owing to the lower dissociation energy of Li-S bond. Sulfur-lithium iron phosphate composites were synthesized by various processes such as solvothermal method (Okada et al. 2018), sol-gel method (Xu et al. 2016), mechano-fusion process (Seo et al. 2015), and solid state method (Yu et al. 2016). Apart from these common methods of synthesis, sulfur coated LiFePO<sub>4</sub> can be obtained by exposing the precursor with sulfur vapor at 400 °C followed by annealing at 400 °C in vacuum (Park et al. 2012). In 2012, Goodenough et al. (Park et al. 2012) proved the enhancement in the charge transfer ability of LFP cathode on nitrogen and sulfur substitution on the surface of anion. According to the theoretical studies reported, the non-coordinated ferrous and ferric ions on the surface of the LFP inhibit the charge transfer causing a decrease in the electrochemical performance of the electrode. On sulfur substitution, the sulfur stabilizes the antibonding 3-D states forming Fe-S bond. During intercalation Li<sup>+</sup> ion binds on the LFP with a binding energy of 0.18 eV (Park et al. 2012). The sulfur substitution is capable to influence the surface energy levels and the charge transfer kinetics. Later in 2015, experimental studies on the effect of sulfur substitution was proved by enhancement in the capacity retention and electrochemical properties (Seo et al. 2015). In 2016, Guan et al. (Yu et al. 2016) studied sulfur substituted LFP/C cathode to obtain a specific capacitance of 114 mAhg<sup>-1</sup> at current density of 0.2 Ag<sup>-1</sup>. Sulfur doped carbon decorated LFP was reported by Xu et al. (2016) obtaining a capacitance of 163.6 mAhg<sup>-1</sup> at a current rate of 0.1 Ag<sup>-1</sup> with a retention ratio of 99.6% after 20 cycles. Sulfur doping on to LFP in the ratio of Li: Fe: P: S is 2.7: 1: 1: 0.22 gave an optimum result with an enhancement of 131 mAhg<sup>-1</sup> at current density of 0.5 Ag<sup>-1</sup>, whereas undoped LFP was reported to have 120.6 mAhg<sup>-1</sup> (Okada et al. 2018). The electrochemical comparison of sulfur doped LFP and undoped LFP is depicted in Fig. 2.18.

### 2.3.4 Doping

Lattice substitution or doping is an alternative method to improve the electronic conductivity of the LFP. Lattice substitution can be done either in lithium site or in iron site. Doping at the lithium (Li) and iron (Fe) site leads to a reduction in the band gap that enhances the electronic conductivity, but the doping process is highly temperature dependent.

Fe site substitution can be done with Mn, Ni, or Co like species that results in the formation of LiMnPO<sub>4</sub>, LiNiPO<sub>4</sub>, LiCoPO<sub>4</sub> as well as partially substituted

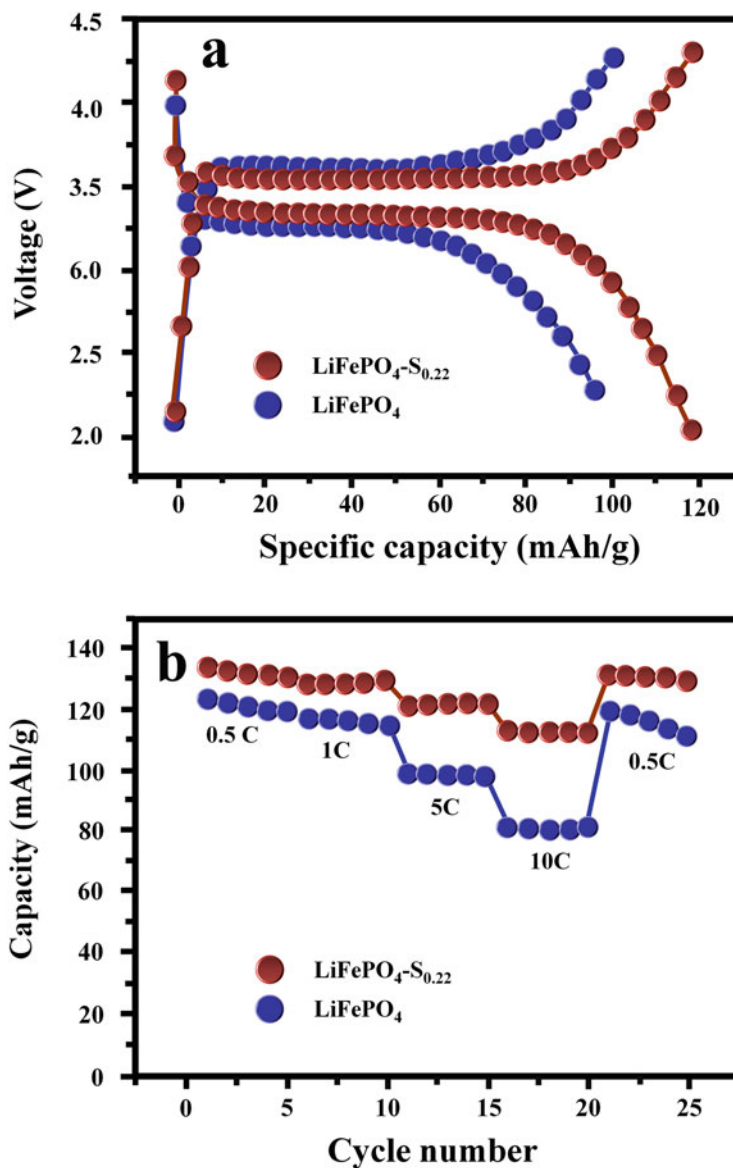


**Fig. 2.18** (a) Charge-discharge curves of LFP and LFP-S<sub>0.22</sub> at 5C, (b) rate performance of LFP and LFP-S<sub>0.22</sub>. (Reprinted with permission of Royal Society of Chemistry from Okada et al. 2018)

compound can also be formed. But due to the energy barrier for the movement of these compounds, the results show a poor property than  $\text{LiFePO}_4$ . The partial substitution of iron ion site is found to be effective in order to improve the bulk conductivity of the olivine compound. Doping with multi-valent cations such as

Al<sup>3+</sup>, Zr<sup>4+</sup>, and Nb<sup>5+</sup> provides an improvement in conductivity compared to that of the former. Compared to mono-valent dopant such as Na<sup>+</sup> at the Li<sup>+</sup>-ion site and M<sup>2+</sup> doping at the Fe<sup>2+</sup> site results in a low favorable energy for Li<sup>+</sup>-ion diffusion. At the same time substitution with the multi-valent cation at both the sites produce an improved conducting property (Fisher et al. 2008). It is found that the improved conductivity of doped olivine structures is not because of the bulk metallic property but due to the formation of a metallic iron phosphide at the surface. During its formation, reduction of LFP to iron phosphide (Fe<sub>2</sub>P) occurs, which induces a metallic conductivity over the LFP grains. Different methods are employed in order to form the dopant olivine structure; based on the synthesis method and temperature condition the effective property of the resultant olivine structure will get varied. Solid state reaction method and one step solid state methods are few of them (Fisher et al. 2008). Solid state reaction method is used for the preparation of Nb<sup>5+</sup> doped LFP and it shows that the ion dopant doesn't depend upon the structural property of LFP (Delacourt et al. 2006; Ban et al. 2012; Molenda et al. 2013).

Substitution of both lithium and iron sites depends strongly on variation in temperature since the solubility of doping decreases with increase in the temperature. Any of the divalent cations can be substituted for either Fe or Li-sites, however, according to the theoretical data multi-valent cations such as Al, Ga, Zr, Ti, Nb, Ta can't be substituted for either Li-site or Fe-site. But later studies show that multi-valent cations are capable to substitute both the Fe site and Li-site (Whittingham 2014). Croce et al. (2002) synthesized LFP with improved property by doping metals like silver and copper only about 1 wt.%. The doped metals improve the kinetics in terms of capacity and cycle life without affecting the structure of LFP.

### 2.3.5 *Size and Morphology*

Grain size and morphology of an electrode material is an important factor that determines its electrochemical performance. The morphology and particle size of LFP particles highly depend on the synthetic parameters such as volume ratio of solvent, reaction temperature, concentration, and feeding rate (Su et al. 2010). The nanosized cathode materials get more attention because of its better electrolyte contact and shorter transport length for both electrons and Li<sup>+</sup>-ions. Nanosized LFP crystals are found in different morphology as nano spindles, nano rods, urchins, nano particles, nano cuboids, and nano flowers (Fig. 2.19).

LFP nano flowers and nano rods reported exhibit superior electrochemical performance and specific capacity. LFP nano rods exhibit predominantly in (010) plane which provide short range pathway for Li<sup>+</sup>-ion transmission. In the case of nano flowers like morphology, diameter of each building block is less than 50 nm. So, the length of the pathway for Li<sup>+</sup>- ion transmission is different for different nano shapes (Nan et al. 2013). Different morphology helps to enhance the electrode–electrolyte interface which not only enhance the charge–discharge rate, but also improve the cycling performance (Bi et al. 2013b).

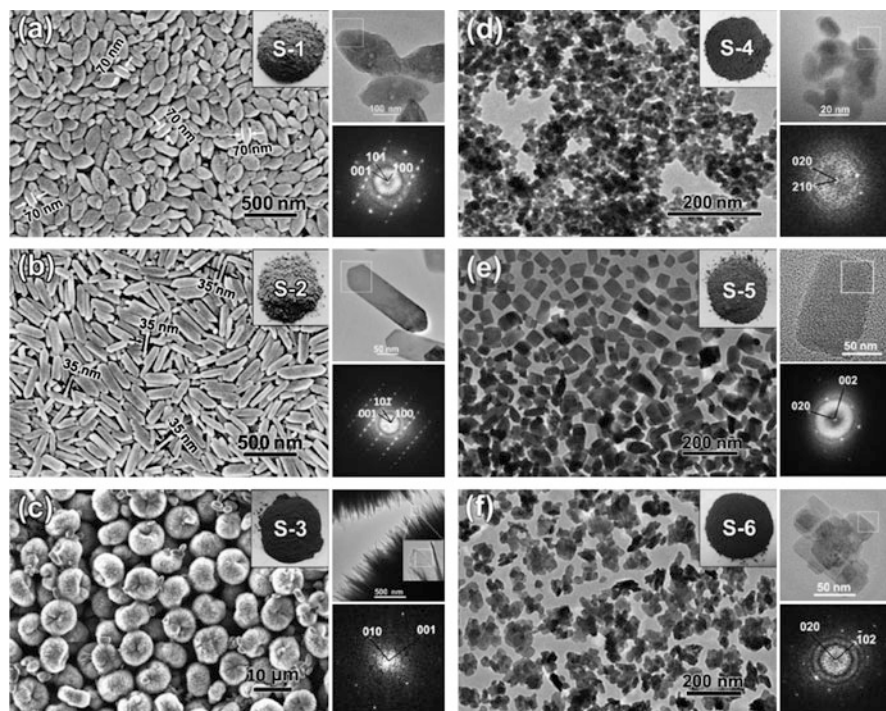


**Fig. 2.19** SEM (left), HRTEM (top-right), and FFT (bottom-right) images of; (a)  $\text{LiFePO}_4$  nanospindles, (b)  $\text{LiFePO}_4$  nanorods, (c)  $\text{LiFePO}_4$  urchins; TEM (left), HRTEM (top-right), and FFT (bottom-right) images of (d)  $\text{LiFePO}_4$  nanoparticles, (e)  $\text{LiFePO}_4$  nanocuboids, and (f)  $\text{LiFePO}_4$  nanoflowers. (Reprinted with permission of Springer Nature from Nan et al. 2013)

## 2.4 Conclusion and Future Outlook

LIBs are the systems that are potentially capable of changing the world. The revolutionary natures of LIBs lead to a huge transformation in battery world. However, some shortcomings make it a questionable technology for the future. The requirement of future batteries that are capable of working in extreme temperatures is important while considering military and space applications. Different research studies are carried out in order to enhance the extreme temperature properties. Being the best cathode, LFP can efficiently be used in variable temperatures with proper modification of the material. Performance of normal batteries appeared to be degrading below  $0^\circ\text{C}$ , but for LFP the electrochemical performance is observed to be efficient. For LFP, the insertion compounds such as  $\text{LiVOPO}_4$  exhibit extremely high temperature performance. While considering the low temperature performance, certain CNT-modified LFP exhibit improved low temperature properties. So, lithium iron phosphate batteries are going to be the future of energy storage



systems that are able to deliver high performance if it can be modified and can be efficiently used even at low and high temperatures.

**Acknowledgments** Author Dr. Jabeen Fatima M. J. would like to acknowledge the Kerala State Council for Science, Technology and Environment (KSCSTE) for financial assistance as post-doctoral research fellowship.

## References

- Ajayan PM, Ebbesen TW (1992) Large-scale synthesis of carbon nanotubes. *Nature* 358:220–222. <https://doi.org/10.1038/358220a0>
- Angela R, Islam H, Sari V et al (2017) Synthesis of LiFePO<sub>4</sub>/C composites based on natural iron stone using a sol gel method. *AIP Conf Proc* 1788:4–8. <https://doi.org/10.1063/1.4968355>
- Bağcı C, Akyıldız O (2018) Synthesis, characterization and electrochemical performance of Nb doped LiFePO<sub>4</sub>/C cathodes. *Hittite J Sci Eng* 5:49–55. <https://doi.org/10.17350/hjse19030000077>
- Ban C, Yin WJ, Tang H et al (2012) A novel codoping approach for enhancing the performance of liFePo 4 cathodes. *Adv Energy Mater* 2:1028–1032. <https://doi.org/10.1002/aenm.201200085>
- Bao L, Xu G, Sun X et al (2017) Mono-dispersed LiFePO<sub>4</sub>@C core-shell [001] nanorods for a high power Li-ion battery cathode. *J Alloys Compd* 708:685–693. <https://doi.org/10.1016/j.jallcom.2017.03.052>
- Benedek P, Wenzler N, Yarema M, Wood VC (2017) Low temperature hydrothermal synthesis of battery grade lithium iron phosphate. *RSC Adv* 7:17763–17767. <https://doi.org/10.1039/c7ra00463j>
- Bi H, Huang F, Tang Y et al (2013a) Study of LiFePO<sub>4</sub> cathode modified by graphene sheets for high-performance lithium ion batteries. *Electrochim Acta* 88:414–420. <https://doi.org/10.1016/j.electacta.2012.10.050>
- Bi Z, Zhang X, He W et al (2013b) Recent advances in LiFePO<sub>4</sub> nanoparticles with different morphology for high-performance lithium-ion batteries. *RSC Adv* 3:19744–19751
- Blomgren GE (2017) The development and future of Lithium ion batteries. *J Electrochem Soc* 164: A5019–A5025. <https://doi.org/10.1149/2.0251701jes>
- Cano ZP, Banham D, Ye S et al (2018) Batteries and fuel cells for emerging electric vehicle markets. *Nat Energy* 3:279–289. <https://doi.org/10.1038/s41560-018-0108-1>
- Chem JM, Zhou X, Wang F, Liu Z (2011) Graphene modified LiFePO<sub>4</sub> cathode materials for high power lithium ion. *J Mater Chem* 21:3353–3358. <https://doi.org/10.1039/c0jm03287e>
- Chen ZY, Zhu HL, Zhu W et al (2010) Electrochemical performance of carbon nanotube-modified LiFePO<sub>4</sub> cathodes for Li-ion batteries. *Trans Nonferrous Met Soc China. English Ed* 20:614–618
- Chen L, Zhang M, Wei W (2013) Graphene-based composites as cathode materials for Lithium ion batteries. *J Nanomater* 2013:8. <https://doi.org/10.1155/2013/940389>
- Chen YT, Zhang HY, Chen YM et al (2018) Graphene-carbon nanotubes-modified LiFePO<sub>4</sub> cathode materials for high-performance lithium-ion batteries. *Mater Sci Forum* 913:818–830. <https://doi.org/10.4028/www.scientific.net/msf.913.818>
- Croce F, D' Epifanio A, Hassoun J et al (2002) A novel concept for the synthesis of an improved LiFePO<sub>4</sub> lithium battery cathode. *Electrochem Solid-State Lett* 5:A47. <https://doi.org/10.1149/1.1449302>
- Cui Y, Zhao X, Guo R (2010) Enhanced electrochemical properties of LiFePO<sub>4</sub> cathode material by CuO and carbon co-coating. *J Alloys Compd* 490:236–240. <https://doi.org/10.1016/j.jallcom.2009.09.165>

- Delacourt C, Wurm C, Laffont L et al (2006) Electrochemical and electrical properties of Nb- and/or C-containing LiFePO<sub>4</sub> composites. *Solid State Ionics* 177:333–341. <https://doi.org/10.1016/j.ssi.2005.11.003>
- Dhindsa KS, Mandal BP, Bazzi K et al (2013a) Enhanced electrochemical performance of graphene modified LiFePO<sub>4</sub> cathode material for lithium ion batteries. *Solid State Ionics* 253:94–100. <https://doi.org/10.1016/j.ssi.2013.08.030>
- Dhindsa KS, Mandal BP, Bazzi K et al (2013b) Enhanced electrochemical performance of graphene modified LiFePO<sub>4</sub> cathode material for lithium ion batteries. *Solid State Ionics* 253:94–100. <https://doi.org/10.1016/j.ssi.2013.08.030>
- Ding Y, Jiang Y, Xu F et al (2010) Preparation of nano-structured LiFePO<sub>4</sub>/graphene composites by co-precipitation method. *Electrochem Commun* 12:10–13. <https://doi.org/10.1016/j.elecom.2009.10.023>
- Feng W, Cao Y, Zhao X et al (2017) Effect of carbon nanotubes on the electrochemical performance of LiFePO<sub>4</sub> particles in lithium ion batteries. *Int J Electrochem Sci* 12:5199–5207. <https://doi.org/10.20964/2017.06.07>
- Fisher CAJ, Prieto VMH, Islam MS (2008) Lithium battery materials LiMPO<sub>4</sub> (M = Mn, Fe, Co, and Ni): insights into defect association, transport mechanisms, and doping behavior. *Chem Mater* 20:5907–5915. <https://doi.org/10.1021/cm801262x>
- Gariépy V, Vediappan K, JT C, Gagnon F, Barray P, Hovington A, Guerfi K, Zaghbi A, Mauger CMJ (2012) Novel hydrothermal synthesis of Nano-LiFePO<sub>4</sub> via solution steering. *Electrochem Soc* 152:2199
- Goodenough JB (2018) How we made the Li-ion rechargeable battery. *Nat Electron* 1:204–204. <https://doi.org/10.1038/s41928-018-0048-6>
- Ha SH, Lee YJ (2015) Core-shell LiFePO<sub>4</sub>/carbon-coated reduced graphene oxide hybrids for high-power lithium-ion battery cathodes. *Chem A Eur J* 21:2132–2138. <https://doi.org/10.1002/chem.201404952>
- Herle PS, Ellis B, Coombs N, Nazar LF (2004) Nano-network electronic conduction in iron and nickel olivine phosphates. *Nat Mater* 3:147–152. <https://doi.org/10.1038/nmat1063>
- Huang C, Ai D, Wang L, He X (2013) Rapid synthesis of LiFePO<sub>4</sub> by Coprecipitation. *Chem Lett* 42:1191–1193. <https://doi.org/10.1246/cl.130436>
- Huang X, Du Y, Qu P et al (2017) Effect of carbon coating on the properties and electrochemical performance of LiFePO<sub>4</sub>/C composites by vacuum decomposition method. *Int J Electrochem Sci* 12:7183–7196. <https://doi.org/10.20964/2017.08.77>
- Iijima S, Ajayan PM, Ichihashi T (1992) Growth model for carbon nanotubes. *Phys Rev Lett* 69:3100–3103. <https://doi.org/10.1103/PhysRevLett.69.3100>
- Islam M, Yoon M, Min Y, Ur S (2015) Solid state synthesis of LiFePO<sub>4</sub>/C: using low cost materials. *J Ceram Process Res* 16:218–222. [https://doi.org/JCPR16-2/\\_082013-034\\_218-222](https://doi.org/JCPR16-2/_082013-034_218-222)
- Jabeen S, Kausar A, Muhammad B et al (2015) A review on polymeric Nanocomposites of Nanodiamond, carbon nanotube, and Nanobifiller: structure, preparation and properties. *Polym Plast Technol Eng* 54:1379–1409. <https://doi.org/10.1080/03602559.2015.1021489>
- Jiang W, Wu M, Liu F et al (2017) Variation of carbon coatings on the electrochemical performance of LiFePO<sub>4</sub> cathodes for lithium ionic batteries. *RSC Adv* 7:44296–44302. <https://doi.org/10.1039/c7ra08062j>
- Jin B, Jin EM, Park KH, Gu HB (2008) Electrochemical properties of LiFePO<sub>4</sub>-multiwalled carbon nanotubes composite cathode materials for lithium polymer battery. *Electrochem Commun* 10:1537–1540. <https://doi.org/10.1016/j.elecom.2008.08.001>
- Julien CM (2017) Lithium Iron phosphate: olivine material for high power Li-ion batteries. *Res Dev Mater Sci* 2:3–6. <https://doi.org/10.31031/rdms.2017.02.000545>
- Kashi R, Khosravi M, Mollazadeh M (2018) Effect of carbon precursor on electrochemical performance of LiFePO<sub>4</sub>-C nano composite synthesized by ultrasonic spray pyrolysis as cathode active material for Li ion battery. *Mater Chem Phys* 203:319–332. <https://doi.org/10.1016/j.matchemphys.2017.10.021>

- Kim HJ, Bae GH, Lee SM et al (2019) Properties of lithium iron phosphate prepared by biomass-derived carbon coating for flexible lithium ion batteries. *Electrochim Acta* 300:18–25. <https://doi.org/10.1016/j.electacta.2019.01.057>
- Konarova M, Taniguchi I (2008) Preparation of LiFePO<sub>4</sub>/C composite powders by ultrasonic spray pyrolysis followed by heat treatment and their electrochemical properties. *Mater Res Bull* 43:3305–3317. <https://doi.org/10.1016/j.materresbull.2008.02.014>
- Kroto HW, Heath JR, O'Brien SC, Curl RF, Smalley RE (1985) C<sub>60</sub>: Buckminsterfullerene. *Nature* 318:162–163. <https://doi.org/10.1038/318162a0>
- Landi BJ, Ganter MJ, Cress CD et al (2009) Carbon nanotubes for lithium ion batteries. *Energy Environ Sci* 2:638–654. <https://doi.org/10.1039/b904116h>
- Lei X, Zhang H, Chen Y, Wang W, Huang Z (2014) Hydrothermal synthesis and electrochemical performance of LiFePO<sub>4</sub> graphene composites for lithium-ion batteries. *Adv Mater Res* 900:242–246. <https://doi.org/10.4028/www.scientific.net/AMR.900.242>
- Li H, Zhou H (2012) Enhancing the performances of Li-ion batteries by carbon-coating: present and future. *Chem Commun* 48:1201–1217. <https://doi.org/10.1039/c1cc14764a>
- Li X, Kang F, Bai X, Shen W (2007) A novel network composite cathode of LiFePO<sub>4</sub>/multiwalled carbon nanotubes with high rate capability for lithium ion batteries. *Electrochem Commun* 9:663–666. <https://doi.org/10.1016/j.elecom.2006.10.050>
- Li L, Li X, Wang Z et al (2009) Stable cycle-life properties of Ti-doped LiFePO<sub>4</sub> compounds synthesized by co-precipitation and normal temperature reduction method. *J Phys Chem Solids* 70:238–242. <https://doi.org/10.1016/j.jpcs.2008.10.012>
- Li YD, Zhao SX, Nan CW, Li BH (2011) Electrochemical performance of SiO<sub>2</sub>-coated LiFePO<sub>4</sub> cathode materials for lithium ion battery. *J Alloys Compd* 509:957–960. <https://doi.org/10.1016/j.jallcom.2010.08.154>
- Lin HY, Yeh SM, Chen JS (2014) Physical and electrochemical properties of LiFePO<sub>4</sub>/C nanofibers synthesized by electrospinning. *Int J Electrochem Sci* 9:6936–6948
- Liu Z, Huang X, Wang D (2008) First-principle investigations of N doping in LiFePO<sub>4</sub>. *Solid State Commun* 147:505–509. <https://doi.org/10.1016/j.ssc.2008.06.013>
- Liu Y, Cao C, Li J (2010) Enhanced electrochemical performance of carbon nanospheres-LiFePO<sub>4</sub> composite by PEG based sol-gel synthesis. *Electrochim Acta* 55:3921–3926. <https://doi.org/10.1016/j.electacta.2010.02.032>
- Liu Y, Liu J, Wang J et al (2018) Formation of size-dependent and conductive phase on lithium iron phosphate during carbon coating. *Nat Commun* 9:1–8. <https://doi.org/10.1038/s41467-018-03324-7>
- Lu L, Han X, Li J et al (2013) A review on the key issues for lithium-ion battery management in electric vehicles. *J Power Sources* 226:272–288. <https://doi.org/10.1016/j.jpowsour.2012.10.060>
- Lung-Hao Hu B, Wu FY, Lin CT et al (2013) Graphene-modified LiFePO<sub>4</sub> cathode for lithium ion battery beyond theoretical capacity. *Nat Commun* 4:1687. <https://doi.org/10.1038/ncomms2705>
- Ma Y, Li X, Sun S et al (2013) Synthesize of graphene-LiFePO<sub>4</sub> composite porous microsphere with the enhanced rate performance. *Int J Electrochem Sci* 8:2842–2848
- Magasinski A, Dixon P, Hertzberg B et al (2010) High-performance lithium-ion anodes using a hierarchical bottom-up approach. *Nat Mater* 9:353–358. <https://doi.org/10.1038/nmat2725>
- Mao S, Pu H, Chen J (2012) Graphene oxide and its reduction: modeling and experimental progress. *RSC Adv* 2:2643–2662. <https://doi.org/10.1039/c2ra00663d>
- May GJ, Davidson A, Monahov B (2018) Lead batteries for utility energy storage: a review. *J Energy Storage* 15:145–157. <https://doi.org/10.1016/j.est.2017.11.008>
- Mizushima K, Jones PC, Wiseman PJ, Goodenough JB (1981) Li<sub>x</sub>CoO<sub>2</sub> (0 < x ≤ 1): a new cathode material for batteries of high energy density. *Solid State Ionics* 3–4:171–174. [https://doi.org/10.1016/0167-2738\(81\)90077-1](https://doi.org/10.1016/0167-2738(81)90077-1)
- Molenda J, Kulka A, Milewska A et al (2013) Structural, transport and electrochemical properties of liFePO<sub>4</sub> substituted in lithium and iron sublattices (Al, Zr, W, Mn, Co and Ni). *Materials (Basel)* 6:1656–1687. <https://doi.org/10.3390/ma6051656>

- Nan C, Lu J, Li L et al (2013) Size and shape control of LiFePO<sub>4</sub> nanocrystals for better lithium ion battery cathode materials. *Nano Res* 6:469–477. <https://doi.org/10.1007/s12274-013-0324-8>
- Naoki N, Feixiang W, Tae LJ, Gleb Y (2015) A new cathode material for batteries of high-energy density. *Mater Today* 18:252–264. <https://doi.org/10.1016/j.mattod.2014.10.040>
- Nishimura SI, Nakamura M, Natsui R, Yamada A (2010) New lithium iron pyrophosphate as 3.5 V class cathode material for lithium ion battery. *J Am Chem Soc* 132:13596–13597. <https://doi.org/10.1021/ja106297a>
- Okada K, Kimura I, Machida K (2018) High rate capability by sulfur-doping into LiFePO<sub>4</sub> matrix. *RSC Adv* 8:5848–5853. <https://doi.org/10.1039/c7ra12740e>
- Padhi AK (1997) Phospho-olivines as positive-electrode materials for rechargeable Lithium batteries. *J Electrochem Soc* 144:1188. <https://doi.org/10.1149/1.1837571>
- Papageorgiou DG, Kinloch IA, Young RJ (2017) Mechanical properties of graphene and graphene-based nanocomposites. *Prog Mater Sci* 90:75–127. <https://doi.org/10.1016/j.pmatsci.2017.07.004>
- Park KS, Son JT, Chung HT et al (2003) Synthesis of LiFePO<sub>4</sub> by co-precipitation and microwave heating. *Electrochem Commun* 5:839–842. <https://doi.org/10.1016/j.elecom.2003.08.005>
- Park KS, Xiao P, Kim SY et al (2012) Enhanced charge-transfer kinetics by anion surface modification of LiFePO<sub>4</sub>. *Chem Mater* 24:3212–3218. <https://doi.org/10.1021/cm301569m>
- Qiao YQ, Feng WL, Li J, Shen TD (2017) Ultralong cycling stability of carbon-nanotube/LiFePO<sub>4</sub> nanocomposites as electrode materials for lithium-ion batteries. *Electrochim Acta* 232:323–331. <https://doi.org/10.1016/j.electacta.2017.02.161>
- Qin X, Wang X, Xiang H et al (2010) Mechanism for hydrothermal synthesis of LiFePO<sub>4</sub> platelets as cathode material for lithium-ion batteries. *J Phys Chem C* 114:16806–16812. <https://doi.org/10.1021/jp104466e>
- Qin G, Ma Q, Wang C (2014a) A porous C/LiFePO<sub>4</sub>/multiwalled carbon nanotubes cathode material for lithium ion batteries. *Electrochim Acta* 115:407–415. <https://doi.org/10.1016/j.electacta.2013.10.177>
- Qin G, Wu Q, Zhao J et al (2014b) C/LiFePO<sub>4</sub>/multi-walled carbon nanotube cathode material with enhanced electrochemical performance for lithium-ion batteries. *J Power Sources* 248:588–595. <https://doi.org/10.1016/j.jpowsour.2013.06.070>
- Qiu Y, Geng Y, Li N et al (2014a) Nonstoichiometric LiFePO<sub>4</sub>/C nano fibers by electrospinning as cathode materials for lithium-ion battery. *Mater Chem Phys* 144:226–229. <https://doi.org/10.1016/j.matchemphys.2013.12.027>
- Qiu Y, Geng Y, Li N et al (2014b) Nonstoichiometric LiFePO<sub>4</sub>/C nanofibers by electrospinning as cathode materials for lithium-ion battery. *Mater Chem Phys* 144:226–229. <https://doi.org/10.1016/j.matchemphys.2013.12.027>
- Rao MC (2015) Novel cathode materials for rechargeable batteries. *Int J Sci Res* 172:637–671. [https://doi.org/10.1007/978-3-319-15458-9\\_23](https://doi.org/10.1007/978-3-319-15458-9_23)
- Ruska M, Kiviluoma J (2011) Challenges in the development of advanced Liion batteries: a review. *Energy Environ Sci*:1–72. <https://doi.org/10.1039/c1ee01598b>
- Salem JR, de Vries MS, Bethune DS et al (2003) Atoms in carbon cages: the structure and properties of endohedral fullerenes. *Nature* 366:123–128. <https://doi.org/10.1038/366123a0>
- Saroha R, Panwar AK (2017) Effect of in situ pyrolysis of acetylene (C<sub>2</sub>H<sub>2</sub>) gas as a carbon source on the electrochemical performance of LiFePO<sub>4</sub> for rechargeable lithium-ion batteries. *J Phys D Appl Phys* 50. <https://doi.org/10.1088/1361-6463/aa708c>
- Saw LH, Somasundaram K, Ye Y, Tay AAO (2014) Electro-thermal analysis of Lithium Iron Phosphate battery for electric vehicles. *J Power Sources* 249:231–238. <https://doi.org/10.1016/j.jpowsour.2013.10.052>
- Seo J, Sankarasubramanian S, Kim CS et al (2015) Thermal characterization of Li/sulfur, Li/S-LiFePO<sub>4</sub> and Li/S-LiV<sub>3</sub>O<sub>8</sub> cells using isothermal micro-calorimetry and accelerating rate calorimetry. *J Power Sources* 289:1–7. <https://doi.org/10.1016/j.jpowsour.2015.04.149>

- Shao D, Wang J, Dong X et al (2013) Electrospinning fabrication and electrochemical properties of LiFePO<sub>4</sub>/C composite nanofibers. *J Mater Sci Mater Electron* 24:4263–4269. <https://doi.org/10.1007/s10854-013-1395-8>
- Su FY, You C, He YB et al (2010) Flexible and planar graphene conductive additives for lithium-ion batteries. *J Mater Chem* 20:9644–9650. <https://doi.org/10.1039/c0jm01633k>
- Susantyoko RA, Karam Z, Alkhoori S et al (2017) A surface-engineered tape-casting fabrication technique toward the commercialisation of freestanding carbon nanotube sheets. *J Mater Chem A* 5:19255–19266. <https://doi.org/10.1039/c7ta04999d>
- Susantyoko RA, Alkindi TS, Kanagaraj AB et al (2018) Performance optimization of freestanding MWCNT-LiFePO<sub>4</sub> sheets as cathodes for improved specific capacity of lithium-ion batteries. *RSC Adv* 8:16566–16573. <https://doi.org/10.1039/c8ra01461b>
- Swain P, Viji M, Mocherla PSV, Sudakar C (2015) Carbon coating on the current collector and LiFePO<sub>4</sub> nanoparticles – influence of sp<sup>2</sup> and sp<sup>3</sup>-like disordered carbon on the electrochemical properties. *J Power Sources* 293:613–625. <https://doi.org/10.1016/j.jpowsour.2015.05.110>
- Świder J, Świątosławski M, Molenda M, Dziembaj R (2014) A novel concept for the synthesis of nanometric LiFePO<sub>4</sub> by co-precipitation method in an anhydrous environment. *Procedia Eng* 98:36–41. <https://doi.org/10.1016/j.proeng.2014.12.484>
- Takahashi M, Tobishima S, Takei K, Sakurai Y (2002) Reaction behavior of LiFePO<sub>4</sub> as a cathode material for rechargeable lithium batteries. *Solid State Ionics* 148:283–289. [https://doi.org/10.1016/S0167-2738\(02\)00064-4](https://doi.org/10.1016/S0167-2738(02)00064-4)
- Tan L, Tang Q, Chen X et al (2014) Mesoporous LiFePO<sub>4</sub> microspheres embedded homogeneously with 3D CNT conductive networks for enhanced electrochemical performance. *Electrochim Acta* 137:344–351. <https://doi.org/10.1016/j.electacta.2014.06.015>
- Tang Y, Huang F, Bi H et al (2012) Highly conductive three-dimensional graphene for enhancing the rate performance of LiFePO<sub>4</sub> cathode. *J Power Sources* 203:130–134. <https://doi.org/10.1016/j.jpowsour.2011.12.011>
- Thanh L, Huynh N, Thuy T et al (2018) Carbon – coated LiFePO<sub>4</sub>– carbon nanotube electrodes for high-rate Li-ion battery. *J Solid State Electrochem* 22:2247–2254. <https://doi.org/10.1007/s10008-018-3934-y>
- Thostenson ET, Ren Z, Chou T (2001) Advances in the science and technology of carbon nanotubes and their composites: a review. *Compos Sci Technol* 61:1899–1912. [https://doi.org/10.1016/S0266-3538\(01\)00094-X](https://doi.org/10.1016/S0266-3538(01)00094-X)
- Tian R, Liu H, Jiang Y et al (2015) Drastically enhanced high-rate performance of carbon-coated LiFePO<sub>4</sub> nanorods using a green chemical vapor deposition (CVD) method for lithium ion battery: a selective carbon coating process. *ACS Appl Mater Interfaces* 7:11377–11386. <https://doi.org/10.1021/acsami.5b01891>
- Toprakci O, Toprakci HAK, Ji L et al (2012) Carbon nanotube-loaded electrospun LiFePO<sub>4</sub>/carbon composite nanofibers as stable and binder-free cathodes for rechargeable lithium-ion batteries. *ACS Appl Mater Interfaces* 4:1273–1280. <https://doi.org/10.1021/am201527r>
- Varzi A, Bresser D, Von Zamory J et al (2014) ZnFe<sub>2</sub>O<sub>4</sub>-C/LiFePO<sub>4</sub>-CNT: a novel high-power lithium-ion battery with excellent cycling performance. *Adv Energy Mater* 4. <https://doi.org/10.1002/aenm.201400054>
- Wang L, Wang H, Liu Z et al (2010) A facile method of preparing mixed conducting LiFePO<sub>4</sub>/graphene composites for lithium-ion batteries. *Solid State Ionics* 181:1685–1689. <https://doi.org/10.1016/j.ssi.2010.09.056>
- Wang Y, Liu Z, Zhou S (2011) An effective method for preparing uniform carbon coated nano-sized LiFePO<sub>4</sub> particles. *Electrochim Acta* 58:359–363. <https://doi.org/10.1016/j.electacta.2011.09.053>
- Wang Y, Feng ZS, Chen JJ, Zhang C (2012) Synthesis and electrochemical performance of LiFePO<sub>4</sub>/graphene composites by solid-state reaction. *Mater Lett* 71:54–56. <https://doi.org/10.1016/j.matlet.2011.12.034>

- Wang S, Yang H, Feng L et al (2013) A simple and inexpensive synthesis route for LiFePO<sub>4</sub>/C nanoparticles by co-precipitation. *J Power Sources* 233:43–46. <https://doi.org/10.1016/j.jpowsour.2013.01.124>
- Wang B, Abdulla WA, Wang D, Zhao XS (2015a) Three-dimensional porous LiFePO<sub>4</sub> cathode material modified with nitrogen-doped graphene aerogel for high-power lithium ion batteries. *Energy Environ Sci* 8:869–875. <https://doi.org/10.1039/b000000x>
- Wang Y, Lv L, Wang J et al (2015b) Influence of microstructure on electrochemical properties of Si/C multilayer thin-film anodes deposited using a sputtering method. *Mater Lett* 160:210–212. <https://doi.org/10.1016/j.matlet.2015.07.084>
- Wang B, Liu T, Liu A et al (2016) A hierarchical porous C@LiFePO<sub>4</sub>/carbon nanotubes microsphere composite for high-rate lithium-ion batteries: combined experimental and theoretical study. *Adv Energy Mater* 6:1600426. <https://doi.org/10.1002/aenm.201600426>
- Wang X, Feng Z, Huang J et al (2018) Graphene-decorated carbon-coated LiFePO<sub>4</sub> nanospheres as a high-performance cathode material for lithium-ion batteries. *Carbon N Y* 127:149–157. <https://doi.org/10.1016/j.carbon.2017.10.101>
- Whittingham MS (2012) History, evolution, and future status of energy storage. *Proc IEEE* 100:1518–1534. <https://doi.org/10.1109/JPROC.2012.2190170>
- Whittingham MS (2014) Ultimate limits to intercalation reactions for Lithium batteries. *Chem Rev* 114:11414–11443. <https://doi.org/10.1021/cr5003003>
- Whittingham MS, Gamble FR (1975) The lithium intercalates of the transition metal dichalcogenides. *Mater Res Bull* 10:363–371. [https://doi.org/10.1016/0025-5408\(75\)90006-9](https://doi.org/10.1016/0025-5408(75)90006-9)
- Wu ZS, Zhou G, Yin LC et al (2012) Graphene/metal oxide composite electrode materials for energy storage. *Nano Energy* 1:107–131. <https://doi.org/10.1016/j.nanoen.2011.11.001>
- Wu G, Zhou Y, Shao Z (2013a) Carbon nanotube and graphene nanosheet co-modified LiFePO<sub>4</sub> nanoplate composite cathode material by a facile polyol process. *Appl Surf Sci* 283:999–1005. <https://doi.org/10.1016/j.apsusc.2013.07.059>
- Wu XL, Guo YG, Su J et al (2013b) Carbonnanotube decorated nano-LiFePO<sub>4</sub> @c cathode material with superior high-rate and low-temperature performances for lithium-ion batteries. *Adv Energy Mater* 3:1155–1160. <https://doi.org/10.1002/aenm.201300159>
- Wu XL, Guo YG, Su J et al (2013c) Carbon-nanotube-decorated nano-LiFePO<sub>4</sub>@C cathode material with superior high-rate and low-temperature performances for lithium-ion batteries. *Adv Energy Mater* 3:1155–1160. <https://doi.org/10.1002/aenm.201300159>
- Xiang JY, Tu JP, Zhang L et al (2010) Improved electrochemical performances of 9LiFePO<sub>4</sub>·Li<sub>3</sub>V<sub>2</sub>(PO<sub>4</sub>)<sub>3</sub>/C composite prepared by a simple solid-state method. *J Power Sources* 195:8331–8335. <https://doi.org/10.1016/j.jpowsour.2010.06.070>
- Xu Z, Xu L, Lai Q, Ji X (2007) A PEG assisted sol-gel synthesis of LiFePO<sub>4</sub> as cathodic material for lithium ion cells. *Mater Res Bull* 42:883–891. <https://doi.org/10.1016/j.materresbull.2006.08.018>
- Xu D, Wang P, Shen B (2016) Synthesis and characterization of sulfur-doped carbon decorated LiFePO<sub>4</sub> nanocomposite as high performance cathode material for lithium-ion batteries. *Ceram Int* 42:5331–5338. <https://doi.org/10.1016/j.ceramint.2015.12.064>
- Yang J, Xu JJ (2004) Nonaqueous sol-gel synthesis of high-performance LiFePO<sub>4</sub>. *Electrochem Solid-State Lett* 7:A515. <https://doi.org/10.1149/1.1819893>
- Yang S, Song Y, Zavalij PY, Stanley Whittingham M (2002) Reactivity, stability and electrochemical behavior of lithium iron phosphates. *Electrochem Commun* 4:239–244. [https://doi.org/10.1016/S1388-2481\(01\)00298-3](https://doi.org/10.1016/S1388-2481(01)00298-3)
- Yang MR, Teng TH, Wu SH (2006) LiFePO<sub>4</sub>/carbon cathode materials prepared by ultrasonic spray pyrolysis. *J Power Sources* 159:307–311. <https://doi.org/10.1016/j.jpowsour.2006.04.113>
- Yang J, Wang J, Wang D et al (2012) 3D porous LiFePO<sub>4</sub> graphene hybrid cathodes with enhanced performance for Li-ion batteries. *J Power Sources* 208:340–344. <https://doi.org/10.1016/j.jpowsour.2012.02.032>
- Yang J, Wang J, Tang Y, Wang D, Li X, Hu Y, Li R, Liang G, Shamb T-K, Sun X (2013) LiFePO<sub>4</sub>-graphene as a superior cathode material for rechargeable lithium batteries: impact of stacked

- graphene and unfolded graphene. *Energy Environ Sci* 6:1521–1528. <https://doi.org/10.1039/C3EE24163G>
- Yang CC, Jang JH, Jiang JR (2015) Preparation of carbon and oxide co-modified LiFePO<sub>4</sub> cathode material for high performance lithium-ion battery. *Mater Chem Phys* 165:196–206. <https://doi.org/10.1016/j.matchemphys.2015.09.018>
- Yu T, Wang Z, Fu Y et al (2016) Sulfur substituted LiFePO<sub>4</sub>/C with improved rate performance for lithium ion batteries. *Int J Electrochem Sci* 11:5999–6008. <https://doi.org/10.20964/2016.07.47>
- Zhang Y, Wang W, Li P et al (2012) A simple solvothermal route to synthesize graphene-modified LiFePO<sub>4</sub> cathode for high power lithium ion batteries. *J Power Sources* 210:47–53. <https://doi.org/10.1016/j.jpowsour.2012.03.007>
- Zhao Y, Li J, Dahn JR (2017) Interdiffusion of Cations from metal oxide surface coatings into LiCoO<sub>2</sub> during sintering. *Chem Mater* 29:5239–5248. <https://doi.org/10.1021/acs.chemmater.7b01219>
- Zhu J, Yoo K, El-Halees I, Kisailus D (2014) Solution deposition of thin carbon coatings on LiFePO<sub>4</sub>. *ACS Appl Mater Interfaces* 6:21550–21557. <https://doi.org/10.1021/am506498p>
- Zou B, Wang Y, Zhou S (2013) Spray drying-assisted synthesis of LiFePO<sub>4</sub>/C composite microspheres with high performance for lithium-ion batteries. *Mater Lett* 92:300–303. <https://doi.org/10.1016/j.matlet.2012.10.111>